Search for dark matter particles in proton-proton collisions at s = 8 √s=8 TeV using the razor variables

Citation: The, C. M. S. collaboration, et al. "Search for Dark Matter Particles in Proton-Proton Collisions at vS=8 Tev Using the Razor Variables." Journal of High Energy Physics 2016 12 (2016).

As Published: 10.1007/JHEP12(2016)088

Publisher: Springer Science and Business Media LLC

Persistent URL: https://hdl.handle.net/1721.1/134598

Version: Final published version: final published article, as it appeared in a journal, conference proceedings, or other formally published context

Published for SISSA by Springer

Received: *March 29, 2016*
Revised: *October 7, 2016*
Accepted: *November 21, 2016*
Published: *December 19, 2016*

Search for dark matter particles in proton-proton collisions at $\sqrt{s} = 8$ TeV using the razor variables

The CMS collaboration

E-mail: cms-publication-committee-chair@cern.ch

Abstract: A search for dark matter particles directly produced in proton-proton collisions recorded by the CMS experiment at the LHC is presented. The data correspond to an integrated luminosity of 18.8 fb^{-1}, at a center-of-mass energy of 8 TeV. The event selection requires at least two jets and no isolated leptons. The razor variables are used to quantify the transverse momentum balance in the jet momenta. The study is performed separately for events with and without jets originating from b quarks. The observed yields are consistent with the expected backgrounds and, depending on the nature of the production mechanism, dark matter production at the LHC is excluded at 90% confidence level for a mediator mass scale Λ below 1 TeV. The use of razor variables yields results that complement those previously published.

Keywords: Hadron-Hadron scattering (experiments), Supersymmetry

ArXiv ePrint: 1603.08914

Article funded by SCOAP^3.

doi:10.1007/JHEP12(2016)088

Contents

1 Introduction **1**

2 The CMS detector **3**

3 Data set and simulated samples **4**

4 Event selection **4**

5 Analysis strategy **6**

6 Background estimation **8**
- 6.1 Background estimation for the zero b-tag search region 8
- 6.2 Background estimation for the 0μb and 0μbb samples 11

7 Systematic uncertainties **14**

8 Results and interpretation **15**
- 8.1 Limits on dark matter production from the 0μ sample 15
- 8.2 Limits on dark matter production from the 0μb and 0μbb samples 18

9 Summary **21**

A Background estimation and observed yield **23**

The CMS collaboration **30**

1 Introduction

The existence of dark matter (DM) in the universe, originally proposed [1] to reconcile observations of the Coma galaxy cluster with the prediction from the virial theorem, is commonly accepted as the explanation of many experimental phenomena in astrophysics and cosmology, such as galaxy rotation curves [2, 3], large structure formation [4–6], and the observed spectrum [7–10] of the cosmic microwave background [11]. A global fit to cosmological data in the ΛCDM model (also known as the standard model of cosmology) [12] suggests that approximately 85% of the mass of the universe is attributable to DM [10]. To accommodate these observations and the dynamics of colliding galaxy clusters [13], it has been hypothesized that DM is made mostly of weakly interacting massive particles (WIMPs), sufficiently massive to be in nonrelativistic motion following their decoupling from the hot particle plasma in the early stages of the expansion of the universe.

While the standard model (SM) of particle physics does not include a viable DM candidate, several models of physics beyond the SM, e.g., supersymmetry (SUSY) [14–18] with R-parity conservation, can accommodate the existence of WIMPs. In these models, pairs of DM particles can be produced in proton-proton (pp) collisions at the CERN LHC. Dark matter particles would not leave a detectable signal in a particle detector. When produced in association with high-energy quarks or gluons, they could provide event topologies with jets and a transverse momentum (p_{T}) imbalance ($\vec{p}_{\mathrm{T}}^{\,\mathrm{miss}}$). The magnitude of $\vec{p}_{\mathrm{T}}^{\,\mathrm{miss}}$ is referred to as missing transverse energy ($E_{\mathrm{T}}^{\mathrm{miss}}$). The ATLAS and CMS collaborations have reported searches for events with one high-p_{T} jet and large $E_{\mathrm{T}}^{\mathrm{miss}}$ [19, 20], which are sensitive to such topologies. In this paper, we refer to these studies as monojet searches. Complementary studies of events with high-p_{T} photons [21, 22]; W, Z, or Higgs bosons [23–26]; b jets [27] and top quarks [27–29]; and leptons [30, 31] have also been performed.

This paper describes a search for dark matter particles χ in events with at least two jets of comparable transverse momenta and sizable $E_{\mathrm{T}}^{\mathrm{miss}}$. The search is based on the razor variables M_R and R^2 [32, 33]. Given a dijet event, these variables are computed from the two jet momenta $\vec{p}^{\,j_1}$ and $\vec{p}^{\,j_2}$, according to the following definition:

$$\begin{aligned} M_R &= \sqrt{(|\vec{p}^{\,j_1}| + |\vec{p}^{\,j_2})^2 - (p_z^{j_1} + p_z^{j_2})^2|}, \\ R &= \frac{M_{\mathrm{T}}^R}{M_R}, \end{aligned} \tag{1.1}$$

with

$$M_{\mathrm{T}}^R = \sqrt{\frac{E_{\mathrm{T}}^{\mathrm{miss}}(p_{\mathrm{T}}^{j_1} + p_{\mathrm{T}}^{j_2}) - \vec{p}_{\mathrm{T}}^{\,\mathrm{miss}} \cdot (\vec{p}_{\mathrm{T}}^{\,j_1} + \vec{p}_{\mathrm{T}}^{\,j_2})}{2}}. \tag{1.2}$$

In the context of SUSY, M_R provides an estimate of the underlying mass scale of the event, and quantity M_{T}^R is a transverse observable that includes information about the topology of the event. The variable R^2 is designed to reduce QCD multijet background; it is correlated with the angle between the two jets, where co-linear jets have large R^2 while back-to-back jets have small R^2. These variables have been used to study the production of non-interacting particles in cascade decays of heavier partners, such as squarks and gluinos in SUSY models with R-parity conservation [34, 35]. The sensitivity of these variables to direct DM production was suggested in ref. [36], where it was pointed out that the dijet event topology provides good discrimination against background processes, with a looser event selection than that applied in the monojet searches. Sensitivity to DM production is most enhanced for large values of R^2, while categorizing events based on the value of M_R improves signal to background discrimination and yields significantly improved search sensitivity to a broader and more inclusive class of DM models. The resulting sensitivity is expected to be comparable to that of monojet searches [36, 37]. This strategy also offers the possibility to search for DM particles that couple preferentially to b quarks [38], as proposed to accommodate the observed excess of photons with energies between 1 and 4 GeV in the gamma ray spectrum of the galactic center data collected by the Fermi-LAT

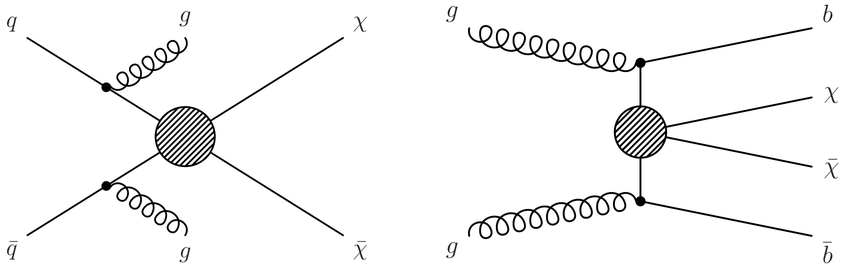

Figure 1. Feynman diagrams for the pair production of DM particles corresponding to an effective field theory using a vector or axial-vector operator (left), and a scalar operator (right).

gamma-ray space telescope [39]. The results are interpreted using an effective field theory approach and the Feynman diagrams for DM pair production are shown in figure 1.

Unlike the SUSY razor searches [33, 35], which focus on events with large values of M_R, this study also considers events with small values of M_R, using R^2 to discriminate between signal and background, in a kinematic region ($R^2 > 0.5$) excluded by the baseline selection of refs. [33, 35].

A data sample corresponding to an integrated luminosity of 18.8 fb^{-1} of pp collisions at a center-of-mass energy of 8 TeV was collected by the CMS experiment with a trigger based on a loose selection on M_R and R^2. This and other special triggers were operated in 2012 to record events at a rate higher than the CMS computing system could process during data taking. The events from these triggers were stored on tape and their reconstruction was delayed until 2013, to profit from the larger availability of processing resources during the LHC shutdown. These data, referred to as "parked data" [40], enabled the exploration of events with small M_R values, thereby enhancing the sensitivity to direct DM production.

This paper is organized as follows: the CMS detector is briefly described in section 2. Section 3 describes the data and simulated samples of events used in the analysis. Sections 4 and 5 discuss the event selections and categorization, respectively. The estimation of the background is described in section 6. The systematic uncertainties are discussed in section 7, while section 8 presents the results and the implications for several models of DM production. A summary is given in section 9.

2 The CMS detector

The central feature of the CMS apparatus is a superconducting solenoid of 6 m internal diameter, providing a magnetic field of 3.8 T. Within the solenoid volume are a silicon pixel and strip tracker, a lead tungstate crystal electromagnetic calorimeter (ECAL), and a brass and scintillator hadron calorimeter (HCAL), each composed of a barrel and two endcap sections. When combining information from the entire detector, the jet energy resolution amounts typically to 15% at 10 GeV, 8% at 100 GeV, and 4% at 1 TeV [41]. Muons are measured in gas-ionization detectors embedded in the steel flux-return yoke outside the solenoid. Forward calorimeters extend the pseudorapidity (η) [42] coverage provided by the barrel and endcap detectors. The first level (L1) of the CMS trigger system, composed of custom hardware processors, uses information from the calorimeters and muon detectors

M_R region (GeV)	200–300	300–400	400–3500
Trigger efficiency (%)	$91.1\pm^{1.5}_{1.7}$	$90.7\pm^{2.3}_{2.9}$	$94.4\pm^{2.4}_{3.6}$

Table 1. Measured trigger efficiency for different M_R regions. The selection $R^2 > 0.35$ is applied. The uncertainty shown represents the statistical uncertainty in the measured efficiency.

to select the most interesting events in a fixed time interval of less than 4 μs. The high-level trigger (HLT) processor farm further decreases the event rate from around 100 kHz to around 400 Hz, before data storage. A more detailed description of the CMS detector, together with a definition of the coordinate system used and the basic kinematic variables, can be found in ref. [42].

3 Data set and simulated samples

The analysis is performed on events with two jets reconstructed at L1 in the central part of the detector ($|\eta| < 3.0$). The L1 jet triggers are based on the sums of transverse energy in regions $\Delta\eta \times \Delta\phi$ approximately 1.05×1.05 in size [42] (where ϕ is the azimuthal angle in the plane transverse to the LHC beams.). At the HLT, energy deposits in ECAL and HCAL are clustered into jets and the razor variables R^2 and M_R are computed. In the HLT, jets are defined using the FastJet [43] implementation of the anti-k_T [44] algorithm, with a distance parameter equal to 0.5. Events with at least two jets with $p_T > 64$ GeV are considered. Events are selected with $R^2 > 0.09$ and $R^2 \times M_R > 45$ GeV. This selection rejects the majority of the background, which tends to have low R^2 and low M_R values, while keeping the events in the signal-sensitive regions of the (M_R, R^2) plane. The trigger efficiency, measured using a pre-scaled trigger with very loose thresholds, is shown in table 1. The requirements described above correspond to the least stringent event selection, given the constraints on the maximum acceptable rate.

Monte Carlo (MC) simulated signal and background samples are generated with the leading order matrix element generator MadGraph v5.1.3 [45, 46] and the CTEQ6L parton distribution function set [47]. The generation includes the pythia 6.4.26 [48] Z2* tune, which is derived from Z1 tune [49] based on the CTEQ5L set. Parton shower and hadronization effects are included by matching the generated events to pythia, using the MLM matching algorithm [50]. The events are processed with a Geant4 [51] description of the CMS apparatus to include detector effects. The simulation samples for SM background processes are scaled to the integrated luminosity of the data sample (18.8 fb^{-1}), using calculations of the inclusive production cross sections at the next-to-next-to-leading order (NNLO) in the perturbative QCD expansion [52–54]. The signal processes corresponding to pair production of DM particles are simulated with up to two additional partons with $p_T > 80$ GeV.

4 Event selection

Events are selected with at least one reconstructed interaction vertex within $|z| < 24$ cm. If more than one vertex is found, the one with the highest sum of the associated track momenta squared is used as the interaction point for event reconstruction. Events containing calorimeter noise, or large missing transverse momentum due to beam halo and instrumental effects (such as jets near non-functioning channels in the ECAL) are removed from the analysis [55].

A particle-flow (PF) algorithm [56, 57] is used to reconstruct and identify individual particles with an optimized combination of information from the various elements of the CMS detector. The energy of photons is directly obtained from the ECAL measurement, corrected for zero-suppression effects. The energy of electrons is determined from a combination of the electron momentum at the primary interaction vertex as measured by the tracker, the energy of the corresponding ECAL cluster, and the energy sum of all bremsstrahlung photons (or emissions) spatially compatible with originating from the electron track. The energy of muons is obtained from the curvature of the associated track. The energy of charged hadrons is determined from a combination of their momentum measured in the tracker and the matching ECAL and HCAL energy deposits, corrected for zero-suppression effects and for the response function of the calorimeters to hadronic showers. Finally, the energy of neutral hadrons is obtained from the corresponding corrected ECAL and HCAL energies. Contamination of the energy determinations from other pp collisions is mitigated by discarding the charged PF candidates incompatible with originating from the main vertex. Additional energy from neutral particles is subtracted on average when computing lepton (electron or muon) isolation and jet energy. This contribution is estimated as the per-event energy deposit per unit area, in the cone $\Delta R = \sqrt{(\Delta\eta)^2 + (\Delta\phi)^2} = 0.3$, times the considered jet size or isolation cone area.

To separate signal from the main backgrounds it is necessary to identify electrons (muons) with $p_{\mathrm{T}} > 15\,\mathrm{GeV}$ and $|\eta| < 2.5$ (2.4). In order to reduce the rate for misidentifying hadrons as leptons, additional requirements based on the quality of track reconstruction and isolation are applied. Lepton isolation is defined as the scalar p_{T} sum of all PF candidates other than the lepton itself, within a cone of size $\Delta R = 0.3$, and normalized to the lepton p_{T}. A candidate is identified as a lepton if the isolation variable is found to be smaller than 15%. For electrons [58], a characteristic of the shower shape of the energy deposit in the ECAL (the shower width in the η direction) is used to further reduce the contamination from hadrons. PF candidates with $p_{\mathrm{T}} > 10\,\mathrm{GeV}$ that are not consistent with muons and satisfy the same isolation requirements as those used for electrons are also identified to increase the lepton selection efficiency as well as to identify single-prong tau decays.

Jets are formed by clustering the PF candidates, using the anti-k_{T} algorithm with distance parameter 0.5. Jet momentum is determined as the vectorial sum of all particle momenta in the jet, and is found from simulation to be within 5% to 10% of the generated hadron level jet momentum over the whole p_{T} spectrum and detector acceptance. Jet energy corrections are derived from simulation, and are confirmed with in situ measurements of the energy balance in dijet and photon+jet events. Any jet whose momentum points within a cone of $\Delta R < 0.3$ around any identified electron, muon, or isolated track is discarded. Additional selection criteria are applied to each event to remove spurious jet-like features originating from isolated noise patterns in certain HCAL regions. We select events containing at least two jets with $p_{\mathrm{T}} > 80\,\mathrm{GeV}$ and $|\eta| < 2.4$, for which the corresponding

L1 and HLT requirements are maximally efficient. The combined secondary vertex (CSV) b-tagging algorithm [59, 60] is used to identify jets originating from b quarks. The loose and tight working points of the CSV algorithm, with 85% (10%) and 50% (0.1%) identification efficiency (misidentification probability) respectively, are used to assign the selected events to categories based on the number of b-tagged jets, as described below.

In order to compute the razor variables inclusively, the event is forced into a two-jet topology, by forming two *megajets* [34] out of all the reconstructed jets with $p_{\mathrm{T}} > 40\,\mathrm{GeV}$ and $|\eta| < 2.4$. All possible assignments of jets to the megajets are considered, with the requirement that a megajet consist of at least one jet. The sum of the four-momenta of the jets assigned to a megajet defines the megajet four-momentum. When more than two jets are reconstructed, more than one megajet assignment is possible. We select the assignment that minimizes the sum of the invariant masses of the two megajets. In order to reduce the contamination from multijet production, events are rejected if the angle between the two selected megajets in the transverse plane $|\Delta\phi(j_1, j_2)|$ is larger than 2.5 radians. The momenta of the two megajets are used to compute the razor variables, according to eq. (1.1), (1.2). Events are required to have $M_R > 200\,\mathrm{GeV}$ and $R^2 > 0.5$.

5 Analysis strategy

To enhance the DM signal and suppress background contributions from the W+jets and $\mathrm{t\bar{t}}$ processes, we veto events with selected electrons, muons, or isolated charged PF candidates. We define three different search regions based on the number of b-tagged jets. The zero b-tag search region contains events where no jets were identified with the CSV loose b-tagging criterion; the one b-tag search region contains events where exactly one jet passed the CSV tight criterion; and the two b-tag search region contains events where two or more jets passed the CSV tight criterion. Events in the zero b-tag search region are further classified into four categories based on the value of M_R, to enhance signal to background discrimination for a broad class of DM models: (i) *very low* M_R (VL), defined by $200 < M_R \leq 300\,\mathrm{GeV}$; (ii) *low* M_R (L), with $300 < M_R \leq 400\,\mathrm{GeV}$; (iii) *high* M_R (H), with $400 < M_R \leq 600\,\mathrm{GeV}$; and (iv) *very high* M_R (VH), including events with $M_R > 600\,\mathrm{GeV}$. Because of the limited size of the data sample, no further categorization based on M_R is made for the one and two b-tag search regions. Within each category, the search is performed in bins of the R^2 variable, with the binning chosen such that the expected background yield in each bin is larger than one event, as estimated from Monte Carlo simulation.

In the H and VH categories, 3% and 35% respectively of the selected events were also selected in the monojet search [61], which used data from the same running period. The overlap in the L and VL categories is negligible, while the overlapping events in the H and VH categories were shown not to have an impact on the final sensitivity. Consequently, the results from this analysis and from the monojet analysis are largely statistically independent.

The main backgrounds in the zero b-tag search region are from the $\mathrm{W}(\ell\nu)$+jets and $\mathrm{Z}(\nu\overline{\nu})$+jets processes, while the dominant background in the one and two b-tag search regions is the $\mathrm{t\bar{t}}$ process. To estimate the contribution of these backgrounds in the search

analysis region	purpose	b-tagging selection	M_R category
0μ	signal search region	no CSV loose jet	$200 < M_R \leq 300\,\text{GeV}$ (VL) $300 < M_R \leq 400\,\text{GeV}$ (L) $400 < M_R \leq 600\,\text{GeV}$ (H) $M_R > 600\,\text{GeV}$ (VH)
1μ	$\text{W}(\ell\nu)$ control region		
2μ	$\text{Z}(\ell\ell)$ control region		

Table 2. Analysis regions for events with zero identified b-tagged jets. The definition of these regions is based on the muon multiplicity, the output of the CSV b-tagging algorithm, and the value of M_R. For all the regions, $R^2 > 0.5$ is required.

analysis region	purpose	b-tagging selection	M_R category
0μbb	signal serach region	$\geq$2 CSV tight jets	$M_R > 200\,\text{GeV}$
0μb		= 1 CSV tight jet	
1μb	$\text{t}\bar{\text{t}}$ control region	$\geq$1 CSV tight jets	
2μb	$\text{t}\bar{\text{t}}$ control region		
$\text{Z}(\mu\mu)$b	$\text{Z}(\ell\ell)$ control region	$\geq$1 CSV loose jets	

Table 3. Analysis regions for events with identified b-tagged jets. The definition of these regions is based on the muon multiplicity, the output of the CSV b-tagging algorithm, and the value of M_R. For all the regions, $R^2 > 0.5$ is required.

regions, we use a data-driven method that extrapolates from appropriately selected control regions to the search region, assisted by Monte Carlo simulation. A detailed description of the background estimation method is discussed in section 6.

To estimate the $\text{W}(\ell\nu)$+jets and $\text{Z}(\nu\overline{\nu})$+jets background in the zero b-tag search region, we define the 1μ control region by selecting events using identical requirements to those used in the search region, with the exception of additionally requiring one selected muon. Events in this control region are extrapolated to the search region in order to estimate the background. In addition, we define the 2μ control region, enhanced in the Z+jets process, by requiring two selected muons with invariant mass between 80 GeV and 100 GeV. The 2μ control region is used to perform a cross-check prediction for the 1μ control region, and the systematic uncertainties in background prediction are estimated based on this comparison.

To estimate the $\text{t}\bar{\text{t}}$ background in the one and two b-tag search regions, we define the 1μb and 2μb control regions, by requiring at least one jet satisfying the CSV tight b-tagging criterion along with one and two selected muons respectively. Both of these control regions are dominated by the $\text{t}\bar{\text{t}}$ process. The $\text{t}\bar{\text{t}}$ background prediction is estimated by extrapolating from the 2μb control region, while the 1μb control region is used as a cross-check to estimate systematic uncertainties. Finally, we define the $\text{Z}(\mu\mu)$b control region by requiring two muons with invariant mass between 80 GeV and 100 GeV. This is used to estimate the $\text{Z}(\nu\overline{\nu})$+jets background in the one and two b-tag search regions.

The definitions of the search and control regions, and their use in this analysis are summarized in tables 2 and 3.

6 Background estimation

The largest background contribution to the zero b-tag search region is from events in which a W or Z boson is produced, in association with jets, decaying to final states with one or more neutrinos. These background processes are referred to as $\mathrm{W}(\ell\nu)$+jets and $\mathrm{Z}(\nu\overline{\nu})$+jets events. Additional backgrounds arise from events involving the production of top quark pairs, and from events in which a Z boson decays to a pair of charged leptons. These processes are referred to as $\mathrm{t\bar{t}}$ and $\mathrm{Z}(\ell\ell)$+jets, respectively. Using simulated samples, the contribution from other SM processes, such as diboson and single top production, is found to be negligible.

The main background in the one and two b-tag search regions comes from $\mathrm{t\bar{t}}$ events. The use of the tight working point of the CSV algorithm reduces the $\mathrm{Z}(\nu\overline{\nu})$+jets and $\mathrm{W}(\ell\nu)$+jets contribution as shown in table 7. Multijet production, which is the most abundant source of events with jets and unbalanced p_{T}, contributes to the search region primarily due to instrumental mismeasurement of the energy of jets. As a result the $E_{\mathrm{T}}^{\mathrm{miss}}$ direction tends to be highly aligned in the azimuthal coordinate with the razor megajets. The requirement on the razor variables and $|\Delta\phi(j_1, j_2)|$ reduces the multijet background to a negligible level, which is confirmed by checking data control regions with looser cuts on the razor variables.

6.1 Background estimation for the zero b-tag search region

To predict the background from $\mathrm{W}(\ell\nu)$+jets and $\mathrm{Z}(\nu\overline{\nu})$+jets in the zero b-tag search region, we use a data-driven method that extrapolates the observed data yields in the 1μ control region to the search region. Similarly, the observed yield in the 2μ control region allows the estimation of the contribution from $\mathrm{Z}(\ell\ell)$+jets background process. Each M_R category is binned in R^2. Events in which the W or Z boson decayed to muons are used to extrapolate to cases where they decay to electrons or taus.

The background expected from W and Z boson production, in each R^2 bin and in each M_R category of the 0μ sample, is computed as

$$\begin{aligned} n_i^{0\mu} = &\left(n_i^{1\mu} - N_i^{\mathrm{t\bar{t}},1\mu} - N_i^{\mathrm{Z}(\ell\ell)\text{+jets},1\mu}\right) \frac{N_i^{\mathrm{W}(\ell\nu)\text{+jets},0\mu} + N_i^{\mathrm{Z}(\nu\overline{\nu})\text{+jets},0\mu}}{N_i^{\mathrm{W}(\ell\nu)\text{+jets},1\mu}} \\ &+\left(n_i^{2\mu} - N_i^{\mathrm{t\bar{t}},2\mu}\right) \frac{N_i^{\mathrm{Z}(\ell\ell)\text{+jets},0\mu}}{N_i^{\mathrm{Z}(\ell\ell)\text{+jets},2\mu}}, \end{aligned} \tag{6.1}$$

where $n_i^{k\mu}$ labels the data yield in bin i for the sample with k muons, and $N_i^{X,k\mu}$ indicates the corresponding yield for process X, derived from simulations. This background estimation method relies on the assumption that the kinematic properties of events in which W and Z bosons are produced are similar.

To estimate the accuracy of the background estimation method, we perform a cross-check by predicting the background in the 1μ control region using the observed data yield in the 2μ control region. The Monte Carlo simulation is used to perform this extrapolation analogous to the calculation in Equation 6.1. The small contribution from the $\mathrm{t\bar{t}}$

M_R category	Z($\nu\overline{\nu}$)+jets	W($\ell\nu$)+jets	Z($\ell\ell$)+jets	$\mathrm{t\overline{t}}$	MC predicted	Estimated	Observed
VL	0.7 ± 0.3	4558 ± 32	133 ± 3	799 ± 9	5491 ± 33	5288 ± 511	5926
L	0.5 ± 0.3	1805 ± 17	44 ± 2	213 ± 4	2063 ± 18	1840 ± 233	2110
H	0.1 ± 0.1	915 ± 11	16 ± 1	66 ± 2	997 ± 11	629 ± 240	923
VH	<0.1	183 ± 5	2.6 ± 0.2	8.5 ± 0.8	194 ± 5	166 ± 93	143

Table 4. Comparison of the observed yield in the 1μ control region in each M_R category and the corresponding data-driven background estimate obtained by extrapolating from the 2μ control region. The uncertainty in the estimates takes into account both the statistical and systematic components. The contribution of each individual background process is also shown, as estimated from simulated samples, as well as the total MC predicted yield.

M_R category	Z($\nu\overline{\nu}$)+jets	W($\ell\nu$)+jets	Z($\ell\ell$)+jets	$\mathrm{t\overline{t}}$	MC predicted	Observed
VL	<0.1	<0.1	214 ± 4	1.9 ± 0.3	215 ± 4	207
L	<0.1	0.4 ± 0.3	88 ± 2	0.5 ± 0.2	89 ± 2	78
H	<0.1	0.1 ± 0.1	48 ± 1	0.1 ± 0.1	48 ± 1	30
VH	<0.1	<0.1	10 ± 1	0.1 ± 0.1	10 ± 1	7

Table 5. Comparison of the observed yield for the 2μ control region in each M_R category and the corresponding prediction from background simulation. The quoted uncertainty in the prediction reflects only the size of the simulated sample. The contribution of each individual background process is also shown, as estimated from simulated samples.

background process is also estimated using the simulated samples. In tables 4 and 5, the observed yields in the 1μ and 2μ control regions respectively are compared to the estimate derived from data. In tables 4–9, the contribution of each process as predicted directly by simulated samples are also given.

Figure 2 shows the comparison of the R^2 distributions between the observed yield and the data-driven background estimate in the 1μ control region. The observed bin-by-bin difference is propagated as a systematic uncertainty in the data-driven background method, and accounts for the statistical uncertainty in the event yield in the 2μ control region data as well as potential differences in the modeling of the recoil spectra between W+jets and Z+jets processes. Some bins exhibit relatively large uncertainties primarily due to statistical fluctuations in the 2μ control region from which the background is prediction estimated. Though the uncertainties are rather large in fractional terms, sensitivity to DM signal models is still obtained, because of the enhanced signal to background ratio for the bins at large values of R^2.

The $\mathrm{t\overline{t}}$ background is estimated using an analogous data-driven method, where we derive corrections to the Monte Carlo simulation prediction scaled to the $\mathrm{t\overline{t}}$ production cross-section computed to NNLO accuracy [52–54] using data in the 2μb control region for each bin in R^2. The correction is then applied to the simulation prediction for the $\mathrm{t\overline{t}}$ background contribution to the zero b-tag search region. This correction factor reflects potential mismodeling of the recoil spectrum predicted by the Monte Carlo simulation. The contribution of each background process to the 2μb sample, predicted from simulated samples, is given in table 6. The fraction of $\mathrm{t\overline{t}}$ events in the 2μb control sample is ≈95%. Figure 3 shows the comparison of the observed yield and the prediction from simulation,

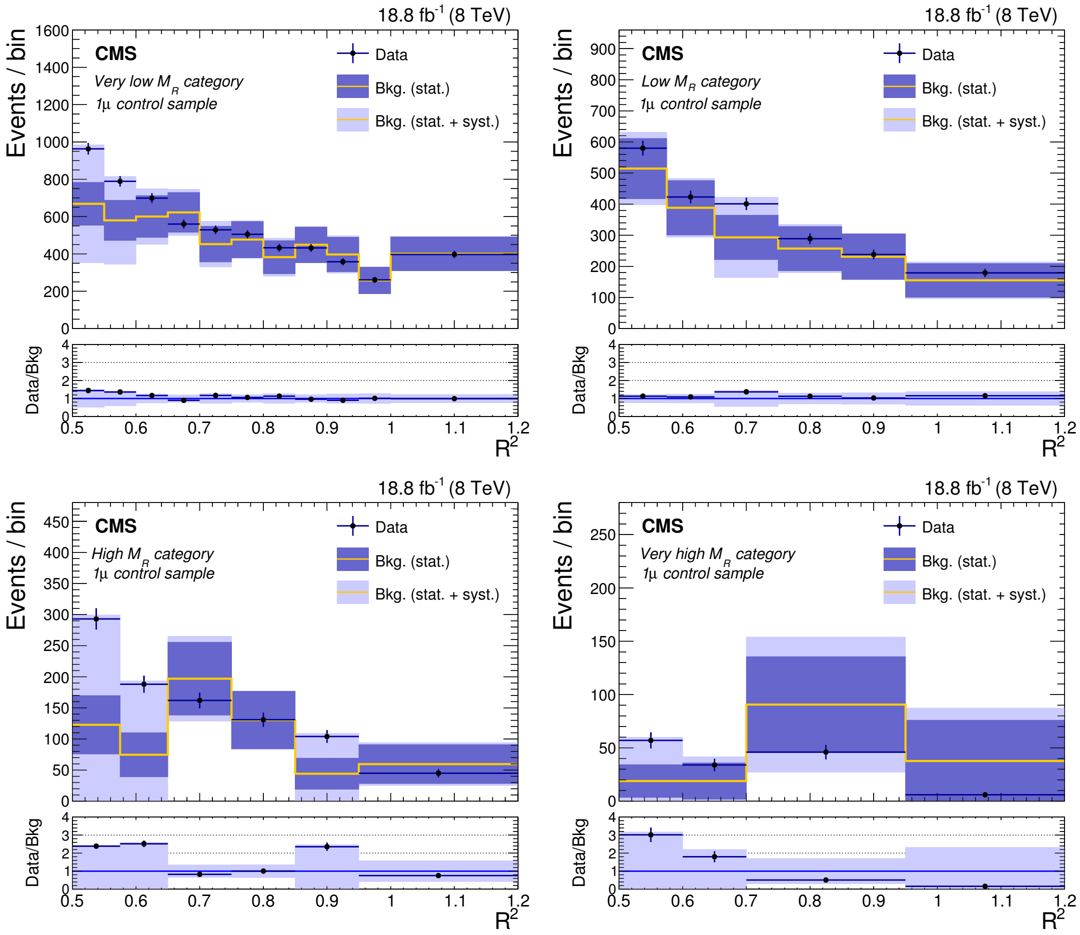

Figure 2. Comparison of observed yields in the 1μ control region and the data-driven background estimate derived from on the 2μ control region data in the four M_R categories: VL (top left), L (top right), H (bottom left), and VH (bottom right). The bottom panel in each plot shows the ratio between the two distributions. The observed bin-by-bin deviation from unity is interpreted as an estimate of the systematic uncertainty associated to the background estimation methodology for the 0μ search region. The dark and light bands represent the statistical and the total uncertainties in the estimates, respectively. The horizontal bars indicate the variable bin widths.

Sample	$Z(\nu\overline{\nu})$+jets	$W(\ell\nu)$+jets	$Z(\ell\ell)$+jets	$t\overline{t}$	MC predicted	Observed
2μb	<0.1	0.1 ± 0.1	2.2 ± 0.3	58 ± 2	60 ± 2	60

Table 6. Observed yield and predicted background from simulated samples in the 2μb control region. The quoted uncertainty in the prediction only reflects the size of the simulated sample. The contribution of each individual background process is also shown, as estimated from simulated samples.

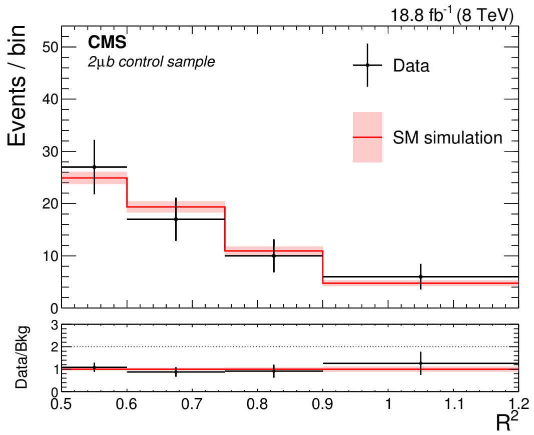

Figure 3. Comparison of the observed yield and the prediction from simulation as a function of R^2 in the 2μb control region. The uncertainties in the data and the simulated sample are represented by the vertical bars and the shaded bands, respectively. The horizontal bars indicate the variable bin widths.

M_R category	Z($\nu\overline{\nu}$)+jets	W($\ell\nu$)+jets	Z($\ell\ell$)+jets	t$\overline{\text{t}}$	MC predicted	Estimated	Observed
VL	6231 ± 37	4820 ± 33	49 ± 2	555 ± 7	11655 ± 50	12770 ± 900	11623
L	2416 ± 19	1513 ± 16	11 ± 1	104 ± 3	4044 ± 25	4170 ± 270	3785
H	1127 ± 7	625 ± 9	2.9 ± 0.3	24 ± 1	1779 ± 12	1650 ± 690	1559
VH	229 ± 2	103 ± 3	0.2 ± 0.1	3.1 ± 0.5	335 ± 3	240 ± 160	261

Table 7. Comparison of the observed yields for for the zero b-tag search region in each M_R category and the corresponding background estimates. The uncertainty in the background estimate takes into account both the statistical and systematic components. The contribution of each individual background process is also shown, as estimated from simulated samples, as well as the total MC predicted yield.

as a function of R^2. We observe no significant deviations between the observed data and the simulation prediction. The uncertainty derived from the data-to-simulation correction factor is propagated to the systematic uncertainty of the t$\overline{\text{t}}$ prediction in the zero b-tag search region.

The result of the background estimation in the zero b-tag search region is given in table 7, where it is compared to the observed yields in data. The uncertainty in the background estimates takes into account both the statistical and systematic components.

The comparison of the data-driven background estimates and the observations for each M_R category is shown in figure 4, as a function of R^2. The expected event distribution is shown for two signal benchmark models, corresponding to the pair production of DM particles of mass 1 GeV in the effective field theory (EFT) approach with vector coupling to u or d quarks. Details on the signal benchmark models are given in section 8.1.

6.2 Background estimation for the 0μb and 0μbb samples

A similar data-driven technique is used to determine the expected background for the one and two b-tag search regions. The background from t$\overline{\text{t}}$ events for each R^2 bin in the one

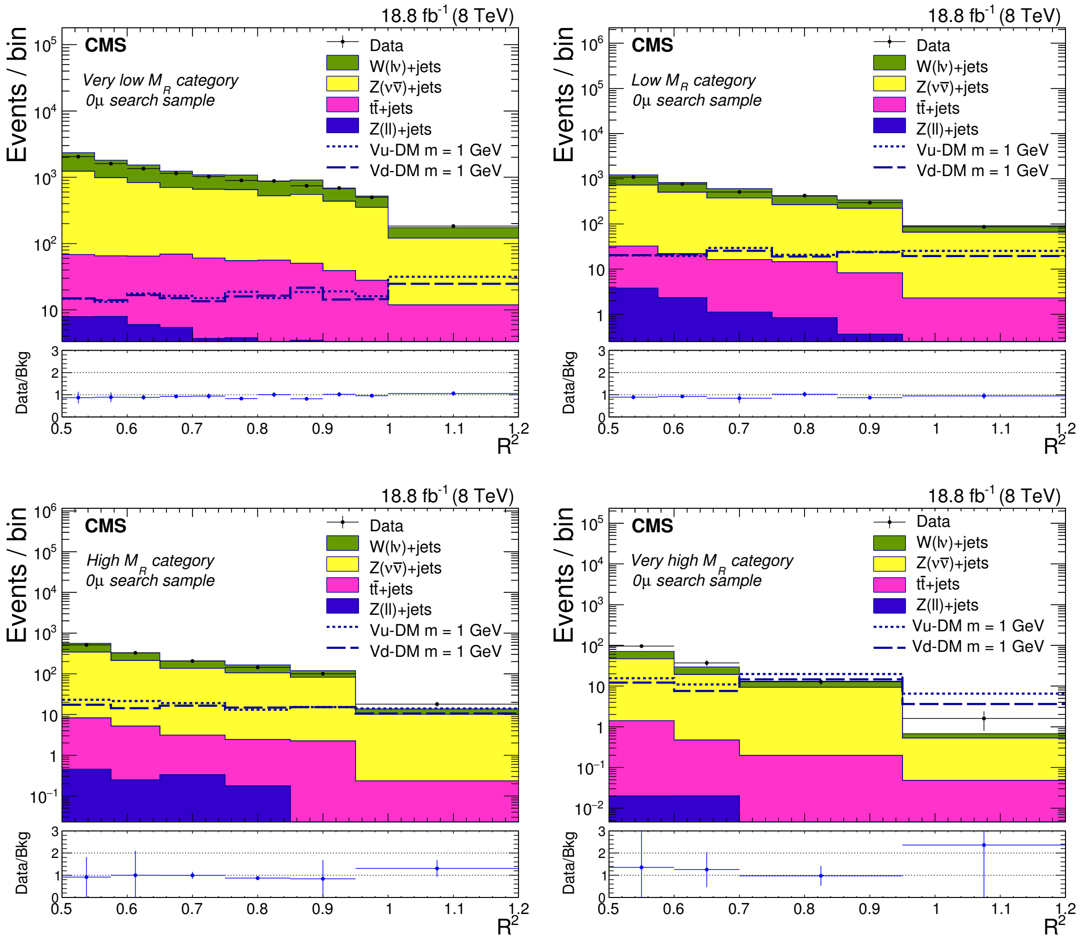

Figure 4. Comparison of the observed yield in the zero b-tag control region and the background estimates in the four M_R categories: VL (top left), L (top right), H (bottom left), and VH (bottom right). The contribution of individual background processes is shown by the filled histograms. The bottom panels show the ratio between the observed yields and the total background estimate. The systematic uncertainty in the ratio includes the systematic uncertainty in the background estimate. For reference, the distributions from two benchmark signal models are also shown, corresponding to the pair production of DM particles of mass 1 GeV in the EFT approach with vector coupling to u or d quarks. The horizontal bars indicate the variable bin widths.

b-tag search region, $n(\mathrm{t\bar{t}})_i^{0\mu\mathrm{b}}$, is computed as:

$$n(\mathrm{t\bar{t}})_i^{0\mu\mathrm{b}} = \left(n(\mathrm{t\bar{t}})_i^{2\mu\mathrm{b}} - N_i^{\mathrm{Z}(\ell\ell)+\mathrm{jets},2\mu\mathrm{b}} - N_i^{\mathrm{W}(\ell\nu)+\mathrm{jets},2\mu\mathrm{b}}\right)\frac{N(\mathrm{t\bar{t}})_i^{0\mu\mathrm{b}}}{N(\mathrm{t\bar{t}})_i^{2\mu\mathrm{b}}} \tag{6.2}$$

where $n(\mathrm{t\bar{t}})_i^{2\mu\mathrm{b}}$ is the observed yield in the ith R^2 bin in the $2\mu\mathrm{b}$ control region, while $N(\mathrm{t\bar{t}})_i^{0\mu\mathrm{b}}$ and $N(\mathrm{t\bar{t}})_i^{2\mu\mathrm{b}}$ are the $\mathrm{t\bar{t}}$ yields in the ith R^2 bin predicted by the simulation for the one b-tag search region and the $2\mu\mathrm{b}$ control region respectively. Similarly, the $\mathrm{t\bar{t}}$ background in the two b-tag search region is derived from eq. (6.2), replacing $N(\mathrm{t\bar{t}})_i^{0\mu\mathrm{b}}$ with $N(\mathrm{t\bar{t}})_i^{0\mu\mathrm{bb}}$, the $\mathrm{t\bar{t}}$ background yield in the ith bin of the two b-tag search region predicted by the simulation. The data yield in the $2\mu\mathrm{b}$ control region is corrected to account for

Sample	$Z(\nu\overline{\nu})$+jets	$W(\ell\nu)$+jets	$Z(\ell\ell)$+jets	$t\bar{t}$	MC predicted	Estimated	Observed
$Z(\mu\mu)$b	<0.1	<0.1	134 ± 3	17 ± 1	151 ± 3	—	175
1μb	0.2 ± 0.1	279 ± 7	11 ± 1	3038 ± 17	3328 ± 18	3410 ± 540	2920

Table 8. Comparison of the observed yields in the $Z(\mu\mu)$b and 1μb samples, the corresponding predictions from background simulation, and (for 1μb only) the cross-check background estimate. The contribution of each individual background process is also shown, as estimated from simulated samples.

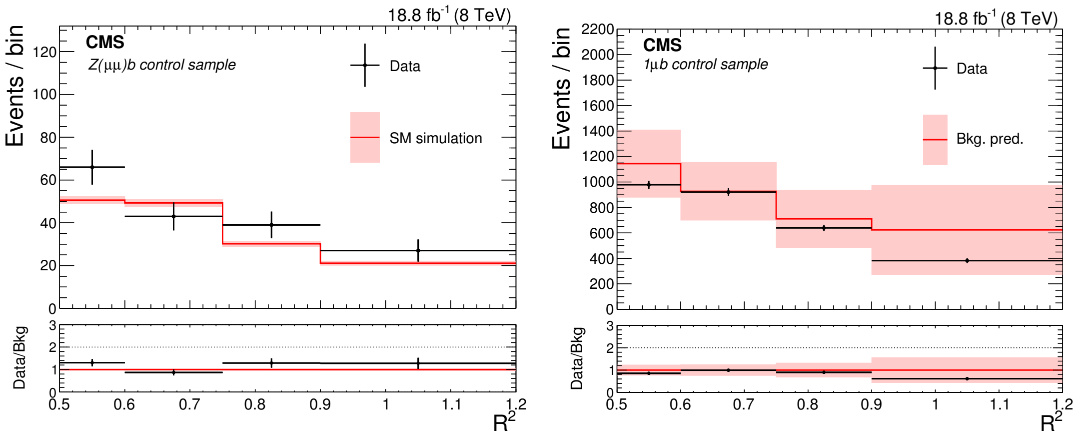

Figure 5. Comparison of the observed yield and the prediction from simulation in the $Z(\mu\mu)$b control sample (left) and of the observed yield in the 1μb control sample and the background estimates from the 2μb and $Z(\mu\mu)$b control samples (right), shown as a function of R^2. The bottom panel of each figure shows the ratio between the data and the estimates. The shaded bands represent the statistical uncertainty in the left plot, and the total uncertainty in the right plot. The horizontal bars indicate the variable bin widths.

the small contamination from Z+jets and W+jets, predicted with the simulated yields $N_i^{Z(\ell\ell)\text{+jets},2\mu\text{b}}$ and $N_i^{W(\ell\nu)\text{+jets},2\mu\text{b}}$, respectively.

The background contribution from $W(\ell\nu)$+jets and $Z(\nu\overline{\nu})$+jets events is predicted using the $Z(\mu\mu)$b control region, and summarized in table 8. The Z+jets purity of this control region is ≈89%. The observed yield in the $Z(\mu\mu)$b control region is shown in the left plot of figure 5, as a function of R^2, along with the Monte Carlo simulation prediction. The uncertainty on the simulation prediction accounts only for the statistical uncertainty of the simulated sample. This contribution, scaled by the ratio of the predicted V+jets background in the search regions to that in the control region, obtained from simulation, provides an estimate for each R^2 bin.

We perform a cross-check of the method on the 1μb control region by predicting the background from the 2μb control region data. The data and prediction are compared on the right of figure 5, where we observe reasonable agreement. The difference between the prediction and the observed data in this cross-check region is propagated as a systematic uncertainty of the method.

The estimated background in the one and two b-tag search regions is given in table 9 and shown in figure 6, where it is compared to the observed yields in data. The uncertainty in the estimates take into account both the statistical and systematic components.

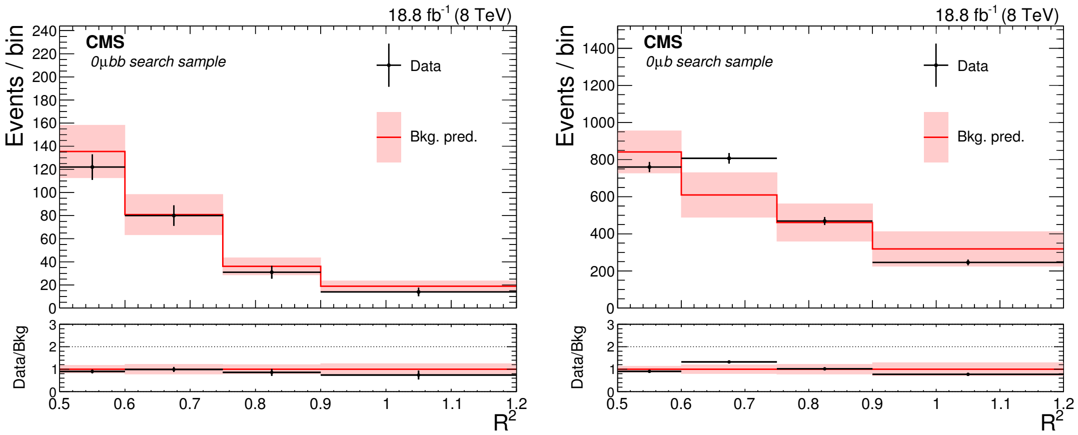

Figure 6. Comparison of observed event yields and background estimates as a function of R^2, for the one (left) and two (right) b-tag search regions. The shaded bands represent the total uncertainty in the estimate. The horizontal bars indicate the variable bin widths.

Sample	$Z(\nu\bar{\nu})$+jets	$W(\ell\nu)$+jets	$Z(\ell\ell)$+jets	$t\bar{t}$	MC predicted	Estimated	Observed
0μbb	44 ± 3	14 ± 2	0.2 ± 0.1	204 ± 4	262 ± 5	271 ± 37	247
0μb	417 ± 8	216 ± 7	2.4 ± 0.4	1480 ± 12	2115 ± 16	2230 ± 280	2282

Table 9. Comparison of the observed yield for events in the one and two b-tag search regions and the corresponding background estimates. The uncertainty in the estimates takes into account both the statistical and systematic components. The contribution of each individual background process is also shown, as estimated from simulated samples, as well as the total MC predicted yield.

7 Systematic uncertainties

For each R^2 bin in each M_R category, the difference between the observed and estimated yields in the crosscheck analysis (see section 6) is taken as the estimate of the uncertainty associated with the method, and covers the differences in the modeling of the recoil spectra between W+jets and Z+jets processes as well as the cross section uncertainties. These uncertainties are found to be typically ≈20–40%, depending on the considered bin in the (M_R, R^2) plane, and are the dominant systematic uncertainties for the analysis. As discussed in section 6.1, a few bins at smaller values of R^2 exhibit larger systematic uncertainties, primarily due to statistical fluctuations in the control region. However the impact on the sensitivity to the dark matter models considered is small as the signal to background ratio is significantly better in other bins at larger values of R^2.

For the 0μ analysis, differences between the kinematic properties of W+jets and Z+jets events are additional sources of systematic uncertainty. These differences arise from the choice of the PDF set, jet energy scale corrections, b tagging efficiency corrections, and trigger efficiency. These effects largely cancel when taking the ratio of the two processes, and the resulting uncertainty is found to be smaller than one fifth of the total uncertainty. The quoted uncertainty is an upper estimate of the total systematic uncertainty.

For the 0μb and 0μbb samples, both the signal and control samples are dominated by $t\bar{t}$ events. The cancellation of the systematic uncertainties is even stronger in this case, since it does not involve different processes, and different PDFs. The remaining uncertainty

Effect	Uncertainty
Jet energy scale	3–6%
Luminosity	2.6%
Parton distribution functions	3–6%
Initial-state radiation	8–15%

Table 10. Systematic uncertainties associated with the description of the DM signal. The values indicated represent the typical size. The dependence of these systematic uncertainties on the R^2 and M_R values is taken into account in the determination of the results.

is dominated by the contribution arising from the small size of the control sample.

Systematic uncertainties in the signal simulation originate from the choice of the PDF set, the jet energy scale correction, the modeling of the initial-state radiation in the event generator, and the uncertainty in the integrated luminosity. The luminosity uncertainty changes the signal normalization while the other uncertainties also modify the signal shape. These effects are taken into account by propagating these uncertainties into the M_R category and the R^2 bin. These uncertainties are considered to be fully correlated across M_R categories and R^2 bins. Typical values for the individual contributions are given in table 10. The total uncertainty in the signal yield is obtained by propagating the individual effects into the M_R and R^2 variables and comparing the bin-by-bin variations with respect to the central value of the prediction based on simulation. In the particular case of the uncertainties due to the choice of the PDF set we have followed the PDF4LHC [62–64] prescription, using the CTEQ-6.6 [65] and MRST-2006-NNLO [66] PDF sets.

8 Results and interpretation

In figures 4 and 6 the estimated backgrounds are compared to the observed yield in each M_R region, for events without and with b-tagged jets, respectively. The background estimates agree with the observed yields, within the uncertainties. This result is interpreted in terms of exclusion limits for several models of DM production.

8.1 Limits on dark matter production from the 0μ sample

The result is interpreted in the context of a low-energy effective field theory, in which the production of DM particles is mediated by six or seven dimension operators [67, 68]. This choice allows the results be compared with those of previous analyses [19, 20], and shows that a similar sensitivity is achieved.

Operators of dimension six and seven are generated assuming the existence of a heavy particle, mediating the interaction between the DM and SM fields. To describe DM production as a local interaction, the propagator of the heavy mediator is expanded through an operator product expansion. The nature of the mediator determines the nature of the effective interaction. Two benchmark scenarios are considered in this study, axial-vector (AV), and vector (V) interactions [69], described by the following operators:

$$\hat{\mathcal{O}}_{\mathrm{AV}} = \frac{1}{\Lambda^2}\,(\bar{\chi}\gamma^{\mu}\gamma_5\chi)\,(\bar{q}\gamma_{\mu}\gamma_5 q)\ \ ; \qquad \hat{\mathcal{O}}_{\mathrm{V}} = \frac{1}{\Lambda^2}\,(\bar{\chi}\gamma^{\mu}\chi)\,(\bar{q}\gamma_{\mu}q)\,. \tag{8.1}$$

Here γ_μ and γ_5 are the Dirac matrices, χ is the DM field, and q is an SM quark field. The DM particle is assumed to be a Dirac fermion where both operators will contribute in the low-energy theory, while in the case of a Majorana DM particle the vector coupling $\hat{\mathcal{O}}_V$ will vanish in the low-energy theory. Below the cutoff energy scale Λ, DM production is described as a contact interaction between two quarks and two DM particles. In the case of s-channel production through a heavy mediator, the energy scale Λ is identified with M/g_{eff}, where M is the mediator mass and $g_{\text{eff}} = \sqrt{g_q g_\chi}$ is an effective coupling, determined by the coupling of the mediator to quark and DM fields, g_q and g_χ, respectively.

The results in tables 14–17 in the appendix are used to obtain an upper limit at 90% confidence level (CL) on the DM production cross section, σ^i_{UL} (where the superscript denotes the coupling to an up or down quark). The limits are obtained using the LHC CL_s procedure [70, 71] and a global likelihood determined by combining the likelihoods of the different search categories. Each systematic uncertainty (see section 7) is incorporated in the likelihood with a dedicated nuisance parameter, whose value is not known a priori but rather must be estimated from the data.

Subsequently, the cross section (σ^i_{UL}) limit is translated into a lower limit Λ_{LL} on the cutoff scale, through the relation:

$$\Lambda_{\text{LL}} = \Lambda_{\text{GEN}} \left(\frac{\sigma_{\text{GEN}}}{\sigma_{\text{UL}}} \right)^{\frac{1}{4}} . \tag{8.2}$$

Here Λ_{GEN} and σ_{GEN} are the cutoff energy scale and cross section of the simulated sample, respectively. The derived values of Λ_{LL} as a function of the DM mass, shown in figure 7, are very similar to those derived for the CMS monojet search [61]. The exclusion limits on Λ weaken at large DM masses since the cross section for DM production is reduced. The analysis has been repeated removing the events also selected by the monojet search. The reduction in background yields due to this additional requirement compensates for the reduction in signal efficiency, resulting in a negligible difference in the exclusion limit on Λ.

The EFT framework provides a benchmark scenario to compare the sensitivity of this analysis with that of previous searches for similar signatures. However, the validity of an EFT approach is limited at the LHC because a fraction of events under study are generated at a $\sqrt{\hat{s}}$ comparable to the cutoff scale Λ [68, 72–74]. For theories to be perturbative, g_{eff} is typically required to be smaller than 4π, and this condition is unlikely to be satisfied for the entire region of phase space probed by the collider searches. In addition, the range of values for the couplings being probed within the EFT may be unrealistically large. Following the study presented in refs. [75–77], we quantify this effect through two EFT validity measures. The first is a minimal kinematic constraint on Λ obtained by requiring $Q_{\text{tr}} < g_{\text{eff}}\Lambda$ and $Q_{\text{tr}} > 2M_\chi$, where Q_{tr} is the momentum transferred from the mediator to the DM particle pair, which yields $\Lambda > 2M_\chi/g_{\text{eff}}$. The second is more stringent and uses the quantity:

$$R_\Lambda = \frac{\int \mathrm{d}R^2 \int \mathrm{d}M_R \left.\dfrac{\mathrm{d}^2\sigma}{\mathrm{d}R^2\mathrm{d}M_R}\right|_{Q_{\text{tr}}<g_{\text{eff}}\Lambda}}{\int \mathrm{d}R^2 \int \mathrm{d}M_R \dfrac{\mathrm{d}^2\sigma}{\mathrm{d}R^2\mathrm{d}M_R}} . \tag{8.3}$$

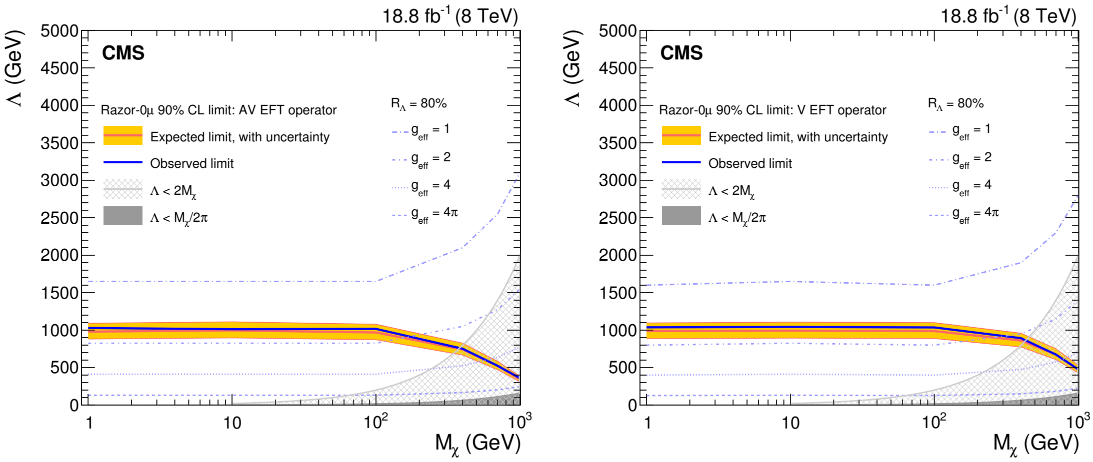

Figure 7. Lower limit at 90% CL on the cutoff scale Λ as a function of the DM mass M_χ in the case of axial-vector (left) and vector (right) currents. The validity of the EFT is quantified by $R_\Lambda = 80\%$ contours, corresponding to different values of the effective coupling g_{eff}. For completeness, regions forbidden by the EFT validity condition $\Lambda > 2M_\chi/g_{\text{eff}}$ are shown for two choices of the effective coupling: $g_{\text{eff}} = 1$ (light gray) and $g_{\text{eff}} = 4\pi$ (dark gray).

Values of R_Λ close to unity indicate a regime in which the assumptions of the EFT approximation hold, while a deviation from unity quantifies the fraction of events for which the EFT approximation is still valid. We consider the case of s-channel production, and we compute R_Λ as a function of the effective coupling g_{eff} in the range $0 < g_{\text{eff}} \leq 4\pi$. The contours corresponding to $R_\Lambda = 80\%$ for different values of g_{eff} are shown in figure 7. For values of $g_{\text{eff}} \gtrsim 2$, the limit set by the analysis lies above the $R_\Lambda = 80\%$ contour.

The exclusion limits on Λ for the axial-vector and vector operators are transformed into upper limits on the spin-dependent ($\sigma^{\text{SD}}_{N\chi}$) [78–84] and spin-independent ($\sigma^{\text{SI}}_{N\chi}$) [80, 81, 85–90] DM-nucleon scattering cross section, respectively; using the following expressions [69]:

$$\sigma^{\text{SD}}_{N\chi} = 0.33\frac{\mu^2}{\pi\Lambda^4_{\text{LL}}}, \tag{8.4}$$

$$\sigma^{\text{SI}}_{N\chi} = 9\frac{\mu^2}{\pi\Lambda^4_{\text{LL}}}, \tag{8.5}$$

where

$$\mu = \frac{M_\chi M_{\text{p}}}{M_\chi + M_{\text{p}}}, \tag{8.6}$$

with M_{p} and M_χ indicating the proton and DM masses, respectively. The numerical values of the derived limits are given in tables 11 and 12. The bound on $\sigma_{N\chi}$ as a function of M_χ is shown in figure 8 for spin-dependent and spin-independent DM-nucleon scattering. A summary of the observed limits for the axial-vector and vector operators can be found in tables 11 and 12 respectively. It is observed that the spin-independent bounds obtained by direct detection experiments are more stringent than those obtained by the present result for masses above $\simeq$ 5 GeV. Such an effect is expected since the spin-independent DM-nucleus cross section is enhanced by the coherent scattering of DM off nucleons in the case

M_χ (GeV)	σ^u_{UL}(pb)	σ^d_{UL}(pb)	Λ_{LL} (GeV)	$\sigma_{N\chi}$ (cm^2)
1	0.39	0.45	1029	8.5×10^{-42}
10	0.43	0.45	1012	2.9×10^{-41}
100	0.30	0.37	1017	3.3×10^{-41}
400	0.25	0.26	752	1.1×10^{-40}
700	0.21	0.26	524	4.7×10^{-40}
1000	0.17	0.22	360	2.1×10^{-39}

Table 11. The 90% CL limits on DM production in the case of axial-vector couplings. Here, σ^u_{UL} and σ^d_{UL} are the observed upper limits on the production cross section for u and d quarks, respectively; Λ_{LL} is the observed cutoff energy scale lower limit; and $\sigma_{N\chi}$ is the observed DM-nucleon scattering cross section upper limit.

M_χ (GeV)	σ^u_{UL}(pb)	σ^d_{UL}(pb)	Λ_{LL} (GeV)	$\sigma_{N\chi}$ (cm^2)
1	0.41	0.38	1038	2.3×10^{-40}
10	0.36	0.45	1043	6.9×10^{-40}
100	0.33	0.44	1036	8.3×10^{-40}
400	0.23	0.35	893	1.5×10^{-39}
700	0.22	0.27	674	4.7×10^{-39}
1000	0.22	0.27	477	1.8×10^{-38}

Table 12. The 90% CL limits on DM production in the case of vector couplings. Here, σ^u_{UL} and σ^d_{UL} are the observed upper limits on the production cross section for u and d quarks, respectively; Λ_{LL} is the observed cutoff energy scale lower limit; and $\sigma_{N\chi}$ is the observed DM-nucleon scattering cross section upper limit.

of spin-independent operators. We note that the present result is more sensitive for small DM mass because the recoil energy in direct detection experiments is lower in this region and therefore more difficult to detect. In the case of spin-dependent DM-nucleus scattering, the present results are more stringent that those obtained by direct detection experiments because the DM-nucleus cross section does not benefit from the coherent enhancement. A summary of the observed limits for the axial-vector and vector operators can be found in tables 11 and 12 respectively.

In order to compare our results with those from direct detection experiments, the experimental bounds in [78–80, 80, 81, 81, 85–88] are translated into bounds on Λ. This comparison is shown in figure 9. This translation is well defined since the momentum transfer in most direct detection experiments is low compared to the values of Λ being probed, and thus the EFT approximations in question are mostly valid.

8.2 Limits on dark matter production from the 0μb and 0μbb samples

The results from the 0μb and 0μbb samples are interpreted in an EFT scenario, following a methodology similar to that of section 8.1. In this case, a heavy scalar mediator is

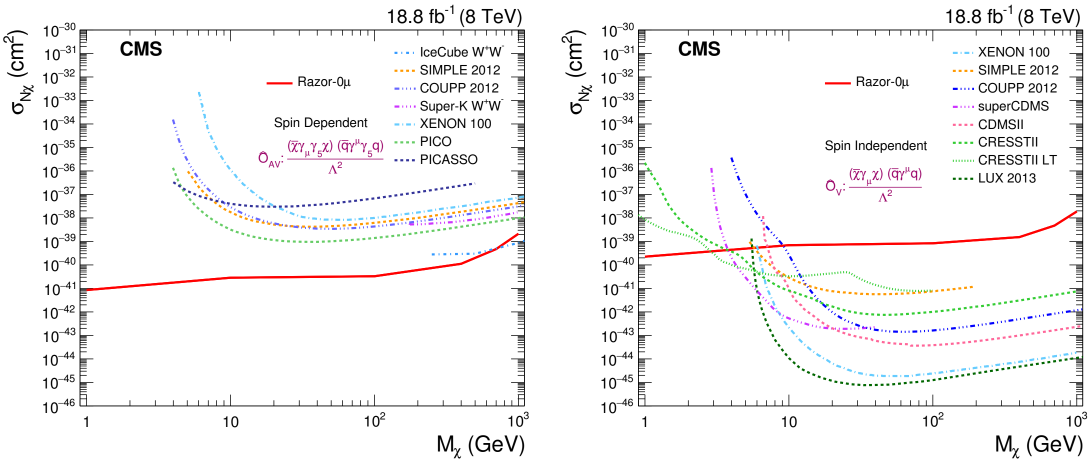

Figure 8. Upper limit at 90% CL on the DM-nucleon scattering cross section $\sigma_{N\chi}$ as a function of the DM mass M_χ in the case of spin-dependent axial-vector (left) and spin-independent vector (right) currents. A selection of representative direct detection experimental bounds are also shown.

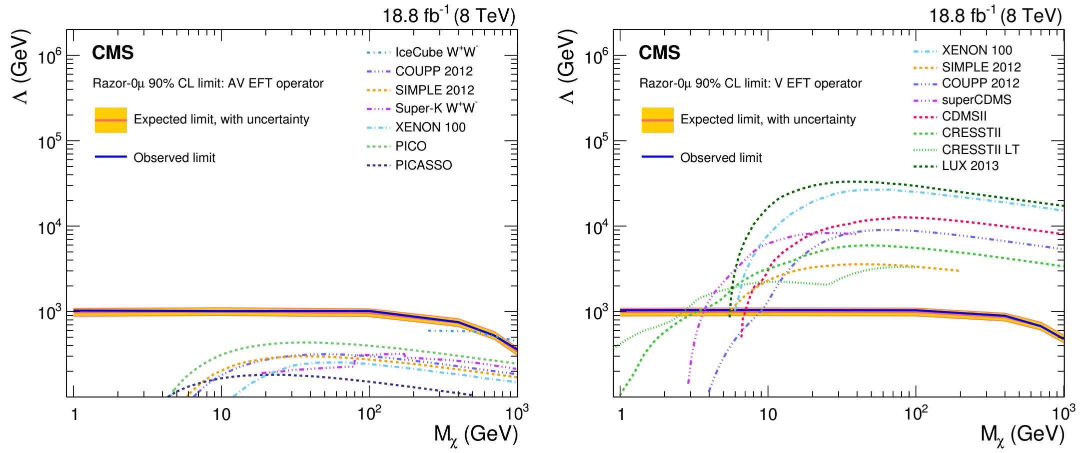

Figure 9. Lower limit at 90% CL on the cutoff scale Λ as a function of the DM mass M_χ in the case of axial-vector (left) and vector (right) currents. A selection of direct detection experimental bounds are also shown.

considered [91], generating an operator:

$$\hat{\mathcal{O}}_S = \frac{M_q}{\Lambda^3}\bar{\chi}\chi\bar{q}q. \tag{8.7}$$

The dependence on the mass, induced by the scalar nature of the mediator, implies a stronger coupling to third-generation quarks, enhancing the sensitivity of the 0μb and 0μbb samples to this scenario. Unlike the case of V and AV operators, the production cross section for this process is proportional to $1/\Lambda^6$. The value of Λ_{LL} is then derived as

$$\Lambda_{\mathrm{LL}} = \Lambda_{\mathrm{GEN}} \left(\frac{\sigma_{\mathrm{GEN}}}{\sigma_{\mathrm{UL}}}\right)^{\frac{1}{6}}. \tag{8.8}$$

Given the results of table 9 we proceed to set limits at 90% CL on the cutoff scale (see table 13) using the LHC CL$_\mathrm{s}$ procedure. To quantify the validity of the EFT we follow the

M_χ (GeV)	$\sigma_{\rm UL}^{\rm obs}$(pb)	$\Lambda_{\rm LL}^{\rm obs}$ (GeV)	$\Lambda_{\rm LL}^{\rm exp}$ (GeV)
0.1	5.4	43.0	48.2
1	3.8	45.3	49.9
10	6.3	43.2	48.4
100	0.8	53.7	55.1
200	0.7	47.2	48.3
300	2.8	32.5	35.8
400	2.8	28.3	30.8
1000	1.7	13.2	13.8

Table 13. The 90% CL limits on DM production in the case of scalar couplings. Here, $\sigma_{\rm UL}^{\rm obs}$ is the observed upper limit on the production cross section, $\Lambda_{\rm LL}^{\rm obs}$ and $\Lambda_{\rm LL}^{\rm exp}$ are the observed and expected cutoff energy scale lower limit, respectively.

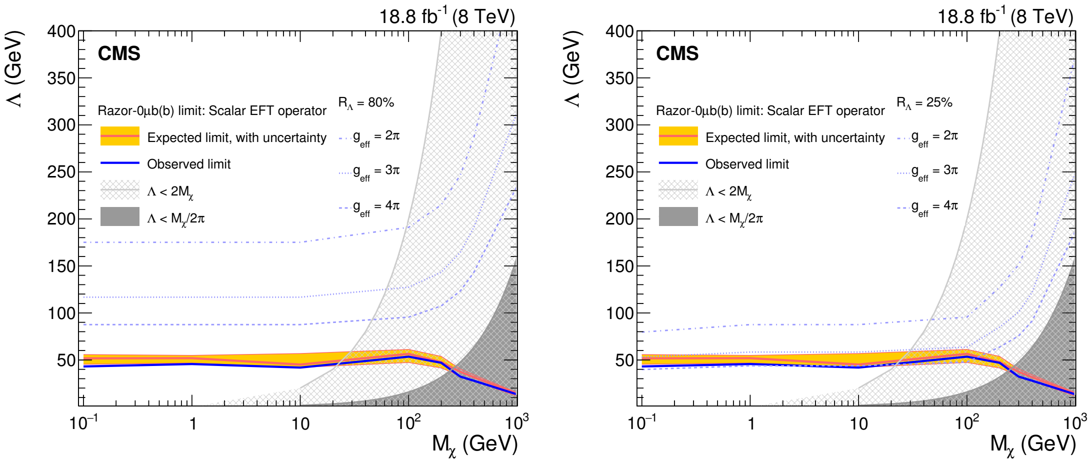

Figure 10. Lower limit at 90% CL on the cutoff scale Λ for the scalar operator $\hat{\mathcal{O}}_S$ as a function of the DM mass M_χ. The validity of the EFT is quantified by $R_\Lambda = 80\%$ (left) and $R_\Lambda = 25\%$ (right) contours, corresponding to different values of the effective coupling $g_{\rm eff}$. For completeness, regions forbidden by the EFT validity condition $\Lambda > 2M_\chi/g_{\rm eff}$ are shown for two choices of the effective coupling: $g_{\rm eff} = 1$ (light gray) and $g_{\rm eff} = 4\pi$ (dark gray).

discussion in section 8.1, considering an interaction mediated by an s-channel produced particle. The operator of eq. (8.7) is suppressed by an additional factor $m_{\rm b}/\Lambda$ with respect to the operators in eq. (8.1). As a result, for a given value of the coupling $g_{\rm eff}$, smaller values of Λ are probed in this case. The observed limit stays below the contours derived for $R_\Lambda = 80\%$, even when the coupling is fixed to the largest value considered, $g_{\rm eff} = 4\pi$, as shown in the left plot of figure 10. For the same choice of coupling, the derived limit on Λ would correspond to $R_\Lambda \approx 25\%$, as shown in the right plot of figure 10. Only for $g_{\rm eff} > 4\pi$ does the observed limit correspond to values of $R_\Lambda > 80\%$. This requirement implies a UV completion of the EFT beyond the perturbative regime. For this reason, this result is not interpreted in terms of an exclusion limit on $\sigma_{N\chi}$.

9 Summary

A search for dark matter has been performed studying proton-proton collisions collected with the CMS detector at the LHC at a center-of-mass energy of 8 TeV. The data correspond to an integrated luminosity of 18.8 fb^{-1}, collected with a dedicated high-rate trigger in 2012, made possible by the creation of parked data, and processed during the LHC shutdown in 2013.

Events with at least two jets are analyzed by studying the distribution in the (M_R, R^2) plane, in an event topology complementary to that of monojet searches. Events with one or two muons are used in conjunction with simulated samples, to predict the expected background from standard model processes, mainly Z+jets and W+jets. The analysis is performed on events both with and without b-tagged jets, originating from the hadronization of a bottom quark, where in the latter case the dominant background comes from $\mathrm{t\bar{t}}$.

No significant excess is observed. The results are presented as exclusion limits on dark matter production at 90% confidence level for models based on effective operators and for different assumptions on the interaction between the dark matter particles and the colliding partons. Dark matter production at the LHC is excluded for a mediator mass scale Λ below 1 TeV in the case of a vector or axial vector operator. While the sensitivity achieved is similar to those of previously published searches, this analysis complements those results since the use of razor variables provides more inclusive selection criteria and since the exploitation of parked data allows events with small values of M_R to be included.

Acknowledgments

We congratulate our colleagues in the CERN accelerator departments for the excellent performance of the LHC and thank the technical and administrative staffs at CERN and at other CMS institutes for their contributions to the success of the CMS effort. In addition, we gratefully acknowledge the computing centers and personnel of the Worldwide LHC Computing Grid for delivering so effectively the computing infrastructure essential to our analyses. Finally, we acknowledge the enduring support for the construction and operation of the LHC and the CMS detector provided by the following funding agencies: the Austrian Federal Ministry of Science, Research and Economy and the Austrian Science Fund; the Belgian Fonds de la Recherche Scientifique, and Fonds voor Wetenschappelijk Onderzoek; the Brazilian Funding Agencies (CNPq, CAPES, FAPERJ, and FAPESP); the Bulgarian Ministry of Education and Science; CERN; the Chinese Academy of Sciences, Ministry of Science and Technology, and National Natural Science Foundation of China; the Colombian Funding Agency (COLCIENCIAS); the Croatian Ministry of Science, Education and Sport, and the Croatian Science Foundation; the Research Promotion Foundation, Cyprus; the Ministry of Education and Research, Estonian Research Council via IUT23-4 and IUT23-6 and European Regional Development Fund, Estonia; the Academy of Finland, Finnish Ministry of Education and Culture, and Helsinki Institute of Physics; the Institut National de Physique Nucléaire et de Physique des Particules / CNRS, and Commissariat à l'Énergie Atomique et aux Énergies Alternatives / CEA, France; the Bundesministerium für

Bildung und Forschung, Deutsche Forschungsgemeinschaft, and Helmholtz-Gemeinschaft Deutscher Forschungszentren, Germany; the General Secretariat for Research and Technology, Greece; the National Scientific Research Foundation, and National Innovation Office, Hungary; the Department of Atomic Energy and the Department of Science and Technology, India; the Institute for Studies in Theoretical Physics and Mathematics, Iran; the Science Foundation, Ireland; the Istituto Nazionale di Fisica Nucleare, Italy; the Ministry of Science, ICT and Future Planning, and National Research Foundation (NRF), Republic of Korea; the Lithuanian Academy of Sciences; the Ministry of Education, and University of Malaya (Malaysia); the Mexican Funding Agencies (CINVESTAV, CONACYT, SEP, and UASLP-FAI); the Ministry of Business, Innovation and Employment, New Zealand; the Pakistan Atomic Energy Commission; the Ministry of Science and Higher Education and the National Science Center, Poland; the Fundação para a Ciência e a Tecnologia, Portugal; JINR, Dubna; the Ministry of Education and Science of the Russian Federation, the Federal Agency of Atomic Energy of the Russian Federation, Russian Academy of Sciences, and the Russian Foundation for Basic Research; the Ministry of Education, Science and Technological Development of Serbia; the Secretaría de Estado de Investigación, Desarrollo e Innovación and Programa Consolider-Ingenio 2010, Spain; the Swiss Funding Agencies (ETH Board, ETH Zurich, PSI, SNF, UniZH, Canton Zurich, and SER); the Ministry of Science and Technology, Taipei; the Thailand Center of Excellence in Physics, the Institute for the Promotion of Teaching Science and Technology of Thailand, Special Task Force for Activating Research and the National Science and Technology Development Agency of Thailand; the Scientific and Technical Research Council of Turkey, and Turkish Atomic Energy Authority; the National Academy of Sciences of Ukraine, and State Fund for Fundamental Researches, Ukraine; the Science and Technology Facilities Council, U.K.; the US Department of Energy, and the US National Science Foundation.

Individuals have received support from the Marie-Curie programme and the European Research Council and EPLANET (European Union); the Leventis Foundation; the A. P. Sloan Foundation; the Alexander von Humboldt Foundation; the Belgian Federal Science Policy Office; the Fonds pour la Formation à la Recherche dans l'Industrie et dans l'Agriculture (FRIA-Belgium); the Agentschap voor Innovatie door Wetenschap en Technologie (IWT-Belgium); the Ministry of Education, Youth and Sports (MEYS) of the Czech Republic; the Council of Science and Industrial Research, India; the HOMING PLUS programme of the Foundation for Polish Science, cofinanced from European Union, Regional Development Fund; the OPUS programme of the National Science Center (Poland); the Compagnia di San Paolo (Torino); MIUR project 20108T4XTM (Italy); the Thalis and Aristeia programmes cofinanced by EU-ESF and the Greek NSRF; the National Priorities Research Program by Qatar National Research Fund; the Rachadapisek Sompot Fund for Postdoctoral Fellowship, Chulalongkorn University (Thailand); the Chulalongkorn Academic into Its 2nd Century Project Advancement Project (Thailand); and the Welch Foundation, contract C-1845; and the Weston Havens Foundation (U.S.A.).

A Background estimation and observed yield

In this section, we provide the background estimate and the observed yield for each bin of the (M_R, R^2) plane.

Tables 14–17 show the expected and observed yields in each R^2 bin of each M_R category for the 0μ sample. Tables 18 and 19 show the corresponding values for the 0μb and the 0μbb samples, respectively.

R^2 range	0.5–0.55	0.55–0.6	0.6–0.65	0.65–0.7
Observed	2049	1607	1352	1147
Estimated	2350 ± 720	1810 ± 450	1530 ± 180	1240 ± 110
R^2 range	0.7–0.75	0.75–0.8	0.8–0.85	0.85–0.9
Observed	1026	896	880	744
Estimated	1090 ± 140	1081 ± 76	876 ± 97	909 ± 63
R^2 range	0.9–0.95	0.95–1.0	1.0–2.5	
Observed	688	499	735	
Estimated	674 ± 67	521 ± 43	694 ± 62	

Table 14. Background estimates and observed yield for each R^2 bin in the VL M_R category.

R^2 range	0.5–0.575	0.575–0.65	0.65–0.75
Observed	1088	765	682
Estimated	1220 ± 120	828 ± 65	810 ± 210
R^2 range	0.75–0.85	0.85–0.95	0.95–2.5
Observed	565	395	290
Estimated	551 ± 59	454 ± 32	304 ± 43

Table 15. Background estimates and observed yield for each R^2 bin in the L M_R category.

R^2 range	0.5–0.575	0.575–0.65	0.65–0.75
Observed	513	328	279
Estimated	560 ± 550	330^{+360}_{-330}	275 ± 41
R^2 range	0.75–0.85	0.85–0.95	0.95–2.5
Observed	203	151	85
Estimated	242 ± 18	171^{+173}_{-171}	74 ± 17

Table 16. Background estimates and observed yield for each R^2 bin in the H M_R category.

R^2 range	0.5–0.6	0.6–0.7	0.7–0.95	0.95–2.5
Observed	117	58	75	11
Estimated	100^{+150}_{-100}	59 ± 36	75 ± 30	9 ± 7

Table 17. Background estimates and observed yield for each R^2 bin in the VH M_R category.

R^2 range	0.5–0.6	0.6–0.75	0.75–0.9	0.9–2.5
Observed	760	807	469	246
Estimated	850 ± 170	620 ± 120	470 ± 110	320 ± 160

Table 18. Background estimates and observed yield for each bin in the 0μb signal region.

R^2 range	0.5–0.6	0.6–0.75	0.75–0.9	0.9–2.5
Observed	122	80	31	14
Estimated	135 ± 30	81 ± 18	36 ± 8	19 ± 9

Table 19. Background estimates and observed yield for each bin in the 0μbb signal region.

References

[1] F. Zwicky, *On the masses of nebulae and of clusters of nebulae*, *Astrophys. J.* **86** (1937) 217 [INSPIRE].

[2] H. C. van de Hulst, E. Raimond, and H. van Woerden, *Rotation and density distribution of the Andromeda nebula derived from observations of the 21 cm line*, *Bull. Astr. Inst. Netherlands* **14** (1957) 1.

[3] V.C. Rubin, N. Thonnard and W.K. Ford Jr., *Rotational properties of 21 SC galaxies with a large range of luminosities and radii, from NGC 4605 $R = 4$ kpc to UGC 2885 $R = 122$ kpc*, *Astrophys. J.* **238** (1980) 471 [INSPIRE].

[4] S.D.M. White, C.S. Frenk, M. Davis and G. Efstathiou, *Clusters, filaments and voids in a universe dominated by cold dark matter*, *Astrophys. J.* **313** (1987) 505 [INSPIRE].

[5] R.G. Carlberg and H.M.P. Couchman, *Mergers and bias in a cold dark matter cosmology*, *Astrophys. J.* **340** (1989) 47.

[6] V. Springel et al., *Simulating the joint evolution of quasars, galaxies and their large-scale distribution*, *Nature* **435** (2005) 629 [`astro-ph/0504097`] [INSPIRE].

[7] COBE collaboration, G.F. Smoot et al., *Structure in the COBE differential microwave radiometer first year maps*, *Astrophys. J.* **396** (1992) L1 [INSPIRE].

[8] BOOMERANG collaboration, *A flat Universe from high resolution maps of the cosmic microwave background radiation*, *Nature* **404** (2000) 955.

[9] WMAP collaboration, D.N. Spergel et al., *Wilkinson Microwave Anisotropy Probe (WMAP) three year results: implications for cosmology*, *Astrophys. J. Suppl.* **170** (2007) 377 [`astro-ph/0603449`] [INSPIRE].

[10] PLANCK collaboration, P.A.R. Ade et al., *Planck 2013 results. XVI. Cosmological parameters*, *Astron. Astrophys.* **571** (2014) A16 [`arXiv:1303.5076`] [INSPIRE].

[11] J.M. Bardeen, J.R. Bond, N. Kaiser and A.S. Szalay, *The statistics of peaks of gaussian random fields*, *Astrophys. J.* **304** (1986) 15 [INSPIRE].

[12] R. Cen, *Decaying cold dark matter model and small-scale power*, *Astrophys. J.* **546** (2001) L77 [`astro-ph/0005206`] [INSPIRE].

[13] D. Clowe et al., *A direct empirical proof of the existence of dark matter*, *Astrophys. J.* **648** (2006) L109 [`astro-ph/0608407`] [INSPIRE].

[14] P. Ramond, *Dual theory for free fermions*, *Phys. Rev.* **D 3** (1971) 2415 [INSPIRE].

[15] Yu. A. Golfand and E.P. Likhtman, *Extension of the algebra of Poincaré group generators and violation of p invariance*, *JETP Lett.* **13** (1971) 323 [INSPIRE].

[16] D.V. Volkov and V.P. Akulov, *Possible universal neutrino interaction*, *JETP Lett.* **16** (1972) 438 [INSPIRE].

[17] J. Wess and B. Zumino, *Supergauge transformations in four-dimensions*, *Nucl. Phys.* **B 70** (1974) 39 [INSPIRE].

[18] P. Fayet, *Supergauge invariant extension of the Higgs mechanism and a model for the electron and its neutrino*, *Nucl. Phys.* **B 90** (1975) 104 [INSPIRE].

[19] ATLAS collaboration, *Search for new phenomena with the monojet and missing transverse momentum signature using the ATLAS detector in* $\sqrt{s} = 7$ *TeV proton-proton collisions*, *Phys. Lett.* **B 705** (2011) 294 [`arXiv:1106.5327`] [INSPIRE].

[20] CMS collaboration, *Search for dark matter and large extra dimensions in monojet events in pp collisions at* $\sqrt{s} = 7$ *TeV*, *JHEP* **09** (2012) 094 [`arXiv:1206.5663`] [INSPIRE].

[21] CMS collaboration, *Search for new phenomena in monophoton final states in proton-proton collisions at* $\sqrt{s} = 8$ *TeV*, *Phys. Lett.* **B 755** (2016) 102 [`arXiv:1410.8812`] [INSPIRE].

[22] ATLAS collaboration, *Search for new phenomena in events with a photon and missing transverse momentum in pp collisions at* $\sqrt{s} = 8$ *TeV with the ATLAS detector*, *Phys. Rev.* **D 91** (2015) 012008 [`arXiv:1411.1559`] [INSPIRE].

[23] ATLAS collaboration, *Search for dark matter in events with a hadronically decaying W or Z boson and missing transverse momentum in pp collisions at* $\sqrt{s} = 8$ *TeV with the ATLAS detector*, *Phys. Rev. Lett.* **112** (2014) 041802 [`arXiv:1309.4017`] [INSPIRE].

[24] ATLAS collaboration, *Search for dark matter in events with a Z boson and missing transverse momentum in pp collisions at* $\sqrt{s} = 8$ *TeV with the ATLAS detector*, *Phys. Rev.* **D 90** (2014) 012004 [`arXiv:1404.0051`] [INSPIRE].

[25] ATLAS collaboration, *Search for dark matter produced in association with a Higgs boson decaying to two bottom quarks in pp collisions at* $\sqrt{s} = 8$ *TeV with the ATLAS detector*, *Phys. Rev.* **D 93** (2016) 072007 [`arXiv:1510.06218`] [INSPIRE].

[26] ATLAS collaboration, *Search for dark matter in events with missing transverse momentum and a Higgs boson decaying to two photons in pp collisions at* $\sqrt{s} = 8$ *TeV with the ATLAS detector*, *Phys. Rev. Lett.* **115** (2015) 131801 [`arXiv:1506.01081`] [INSPIRE].

[27] ATLAS collaboration, *Search for dark matter in events with heavy quarks and missing transverse momentum in pp collisions with the ATLAS detector*, Eur. Phys. J. **C 75** (2015) 92 [`arXiv:1410.4031`] [INSPIRE].

[28] CMS collaboration, *Search for Monotop signatures in proton-proton collisions at $\sqrt{s} = 8$ TeV*, Phys. Rev. Lett. **114** (2015) 101801 [`arXiv:1410.1149`] [INSPIRE].

[29] CMS collaboration, *Search for the production of dark matter in association with top-quark pairs in the single-lepton final state in proton-proton collisions at $\sqrt{s} = 8$ TeV*, JHEP **06** (2015) 121.

[30] ATLAS collaboration, *Search for new particles in events with one lepton and missing transverse momentum in pp collisions at $\sqrt{s} = 8$ TeV with the ATLAS detector*, JHEP **09** (2014) 037 [`arXiv:1407.7494`] [INSPIRE].

[31] CMS collaboration, *Search for physics beyond the standard model in final states with a lepton and missing transverse energy in proton-proton collisions at $\sqrt{s} = 8$ TeV*, Phys. Rev. **D 91** (2015) 092005 [`arXiv:1408.2745`] [INSPIRE].

[32] C. Rogan, *Kinematical variables towards new dynamics at the LHC*, `arXiv:1006.2727` [INSPIRE].

[33] CMS collaboration, *Inclusive search for squarks and gluinos in pp collisions at $\sqrt{s} = 7$ TeV*, Phys. Rev. **D 85** (2012) 012004 [`arXiv:1107.1279`] [INSPIRE].

[34] CMS collaboration, *Search for supersymmetry with razor variables in pp collisions at $\sqrt{s} = 7$ TeV*, Phys. Rev. **D 90** (2014) 112001 [`arXiv:1405.3961`] [INSPIRE].

[35] CMS collaboration, *Search for supersymmetry using razor variables in events with b-tagged jets in pp collisions at $\sqrt{s} = 8$ TeV*, Phys. Rev. **D 91** (2015) 052018 [`arXiv:1502.00300`] [INSPIRE].

[36] P.J. Fox, R. Harnik, R. Primulando and C.-T. Yu, *Taking a razor to dark matter parameter space at the LHC*, Phys. Rev. **D 86** (2012) 015010 [`arXiv:1203.1662`] [INSPIRE].

[37] M. Papucci, A. Vichi and K.M. Zurek, *Monojet versus the rest of the world I: t-channel models*, JHEP **11** (2014) 024 [`arXiv:1402.2285`] [INSPIRE].

[38] P. Agrawal, B. Batell, D. Hooper and T. Lin, *Flavored dark matter and the galactic center gamma-ray excess*, Phys. Rev. **D 90** (2014) 063512 [`arXiv:1404.1373`] [INSPIRE].

[39] D. Hooper and L. Goodenough, *Dark matter annihilation in the galactic center as seen by the Fermi Gamma Ray Space Telescope*, Phys. Lett. **B 697** (2011) 412 [`arXiv:1010.2752`] [INSPIRE].

[40] CMS collaboration, *Data parking and data scouting at the CMS experiment*, CMS-DP-2012-022 (2012).

[41] CMS collaboration, *Energy calibration and resolution of the CMS electromagnetic calorimeter in pp collisions at $\sqrt{s} = 7$ TeV*, 2013 *JINST* **8** P09009 [`arXiv:1306.2016`] [INSPIRE].

[42] CMS collaboration, *The CMS experiment at the CERN LHC*, 2008 *JINST* **3** S08004 [INSPIRE].

[43] M. Cacciari, G.P. Salam and G. Soyez, *FastJet user manual*, Eur. Phys. J. **C 72** (2012) 1896 [`arXiv:1111.6097`] [INSPIRE].

[44] M. Cacciari, G.P. Salam and G. Soyez, *The anti-$k(t)$ jet clustering algorithm*, JHEP **04** (2008) 063 [`arXiv:0802.1189`] [INSPIRE].

[45] J. Alwall, M. Herquet, F. Maltoni, O. Mattelaer and T. Stelzer, *MadGraph 5: going beyond*, *JHEP* **06** (2011) 128 [arXiv:1106.0522] [INSPIRE].

[46] J. Alwall et al., *The automated computation of tree-level and next-to-leading order differential cross sections and their matching to parton shower simulations*, *JHEP* **07** (2014) 079 [arXiv:1405.0301] [INSPIRE].

[47] J. Pumplin, D.R. Stump, J. Huston, H.L. Lai, P.M. Nadolsky and W.K. Tung, *New generation of parton distributions with uncertainties from global QCD analysis*, *JHEP* **07** (2002) 012 [hep-ph/0201195] [INSPIRE].

[48] T. Sjöstrand, S. Mrenna and P.Z. Skands, *PYTHIA 6.4 physics and manual*, *JHEP* **05** (2006) 026 [hep-ph/0603175] [INSPIRE].

[49] R. Field, *Early LHC underlying event data — Findings and surprises*, in the proceedings of the 22nd *Hadron Collider Physics Symposium (HCP 2010)*, August 23–27, Toronto, Canada (2010), arXiv:1010.3558 [INSPIRE].

[50] S. Höche et al., *Matching parton showers and matrix elements*, hep-ph/0602031 [INSPIRE].

[51] GEANT4 collaboration, S. Agostinelli et al., *GEANT4 — A Simulation toolkit*, *Nucl. Instrum. Meth.* **A 506** (2003) 250 [INSPIRE].

[52] R. Gavin, Y. Li, F. Petriello and S. Quackenbush, *W physics at the LHC with FEWZ 2.1*, *Comput. Phys. Commun.* **184** (2013) 208 [arXiv:1201.5896] [INSPIRE].

[53] R. Gavin, Y. Li, F. Petriello and S. Quackenbush, *FEWZ 2.0: a code for hadronic Z production at next-to-next-to-leading order*, *Comput. Phys. Commun.* **182** (2011) 2388 [arXiv:1011.3540] [INSPIRE].

[54] M. Czakon and A. Mitov, *Top++: a program for the calculation of the top-pair cross-section at hadron colliders*, *Comput. Phys. Commun.* **185** (2014) 2930 [arXiv:1112.5675] [INSPIRE].

[55] CMS collaboration, *Performance of the CMS missing transverse momentum reconstruction in pp data at* $\sqrt{s} = 8$ *TeV*, 2015 *JINST* **10** P02006.

[56] CMS collaboration, *Particle-flow event reconstruction in CMS and performance for jets, taus and MET*, CMS-PAS-PFT-09-001 (2009).

[57] CMS collaboration, *Commissioning of the particle-flow event reconstruction with the first LHC collisions recorded in the CMS detector*, CMS-PAS-PFT-10-001 (2010).

[58] CMS collaboration, *Performance of electron reconstruction and selection with the CMS detector in proton-proton collisions at* $\sqrt{s} = 8$ *TeV*, 2015 *JINST* **10** P06005 [arXiv:1502.02701] [INSPIRE].

[59] CMS collaboration, *Performance of b tagging at* $\sqrt{s} = 8$ *TeV in multijet, ttbar and boosted topology events*, CMS-PAS-BTV-13-001 (2013).

[60] CMS collaboration, *Identification of b-quark jets with the CMS experiment*, 2013 *JINST* **8** P04013 [arXiv:1211.4462] [INSPIRE].

[61] CMS collaboration, *Search for dark matter, extra dimensions and unparticles in monojet events in proton-proton collisions at* $\sqrt{s} = 8$ *TeV*, *Eur. Phys. J.* **C 75** (2015) 235 [arXiv:1408.3583] [INSPIRE].

[62] D. Bourilkov, R.C. Group and M.R. Whalley, *LHAPDF: PDF use from the Tevatron to the LHC*, in the proceedings of the *TeV4LHC Workshop — 4th meeting*, October 20–22, Batavia, U.S.A. (2005), hep-ph/0605240 [INSPIRE].

[63] S. Alekhin et al., *The PDF4LHC Working Group Interim Report*, arXiv:1101.0536 [INSPIRE].

[64] M. Botje et al., *The PDF4LHC working group interim recommendations*, arXiv:1101.0538 [INSPIRE].

[65] P.M. Nadolsky et al., *Implications of CTEQ global analysis for collider observables*, *Phys. Rev.* **D 78** (2008) 013004 [arXiv:0802.0007] [INSPIRE].

[66] A.D. Martin, W.J. Stirling, R.S. Thorne and G. Watt, *Update of parton distributions at NNLO*, *Phys. Lett.* **B 652** (2007) 292 [arXiv:0706.0459] [INSPIRE].

[67] M. Beltrán, D. Hooper, E.W. Kolb, Z.A.C. Krusberg and T.M.P. Tait, *Maverick dark matter at colliders*, *JHEP* **09** (2010) 037 [arXiv:1002.4137] [INSPIRE].

[68] Y. Bai, P.J. Fox and R. Harnik, *The Tevatron at the frontier of dark matter direct detection*, *JHEP* **12** (2010) 048 [arXiv:1005.3797] [INSPIRE].

[69] P.J. Fox, R. Harnik, J. Kopp and Y. Tsai, *Missing energy signatures of dark matter at the LHC*, *Phys. Rev.* **D 85** (2012) 056011 [arXiv:1109.4398] [INSPIRE].

[70] ATLAS collaboration, *Procedure for the LHC Higgs boson search combination in summer 2011*, ATL-PHYS-PUB-2011-011 (2011).

[71] ATLAS and CMS collaborations and The LHC Higgs Combination Group, *Procedure for the LHC Higgs boson search combination in Summer 2011*, CMS-NOTE-2011-005 (2011).

[72] J. Goodman, M. Ibe, A. Rajaraman, W. Shepherd, T.M.P. Tait and H.-B. Yu, *Constraints on dark matter from colliders*, *Phys. Rev.* **D 82** (2010) 116010 [arXiv:1008.1783] [INSPIRE].

[73] A. Friedland, M.L. Graesser, I.M. Shoemaker and L. Vecchi, *Probing nonstandard standard model backgrounds with LHC monojets*, *Phys. Lett.* **B 714** (2012) 267 [arXiv:1111.5331] [INSPIRE].

[74] O. Buchmueller, M.J. Dolan and C. McCabe, *Beyond effective field theory for dark matter searches at the LHC*, *JHEP* **01** (2014) 025 [arXiv:1308.6799] [INSPIRE].

[75] G. Busoni, A. De Simone, E. Morgante and A. Riotto, *On the validity of the effective field theory for dark matter searches at the LHC*, *Phys. Lett.* **B 728** (2014) 412 [arXiv:1307.2253] [INSPIRE].

[76] G. Busoni, A. De Simone, J. Gramling, E. Morgante and A. Riotto, *On the validity of the effective field theory for dark matter searches at the LHC, Part II: complete Analysis for the s-channel*, *JCAP* **06** (2014) 060 [arXiv:1402.1275] [INSPIRE].

[77] G. Busoni, A. De Simone, T. Jacques, E. Morgante and A. Riotto, *On the validity of the effective field theory for dark matter searches at the LHC part III: analysis for the t-channel*, *JCAP* **09** (2014) 022 [arXiv:1405.3101] [INSPIRE].

[78] SUPER-KAMIOKANDE collaboration, T. Tanaka et al., *An indirect search for WIMPs in the Sun using 3109.6 days of upward-going muons in Super-Kamiokande*, *Astrophys. J.* **742** (2011) 78 [arXiv:1108.3384] [INSPIRE].

[79] ICECUBE collaboration, R. Abbasi et al., *Multi-year search for dark matter annihilations in the Sun with the AMANDA-II and IceCube detectors*, *Phys. Rev.* **D 85** (2012) 042002 [arXiv:1112.1840] [INSPIRE].

[80] COUPP collaboration, E. Behnke et al., *First dark matter search results from a 4 kg CF_3I bubble chamber operated in a deep underground site*, *Phys. Rev.* **D 86** (2012) 052001 [arXiv:1204.3094] [INSPIRE].

[81] M. Felizardo et al., *Final analysis and results of the phase II SIMPLE dark matter search*, *Phys. Rev. Lett.* **108** (2012) 201302 [arXiv:1106.3014] [INSPIRE].

[82] PICO collaboration, C. Amole et al., *Dark matter search results from the PICO-2L C_3F_8 bubble chamber*, *Phys. Rev. Lett.* **114** (2015) 231302 [`arXiv:1503.00008`] [INSPIRE].

[83] PICASSO collaboration, S. Archambault et al., *Constraints on low-mass WIMP interactions on ^{19}F from PICASSO*, *Phys. Lett.* **B 711** (2012) 153 [`arXiv:1202.1240`] [INSPIRE].

[84] XENON100 collaboration, E. Aprile et al., *Limits on spin-dependent WIMP-nucleon cross sections from* 225 *live days of XENON100 data*, *Phys. Rev. Lett.* **111** (2013) 021301 [`arXiv:1301.6620`] [INSPIRE].

[85] CDMS-II collaboration, *Dark matter search results from the CDMS II experiment*, *Science* **327** (2010) 1619 [*Erratum ibid.* **330** (2010) 1047].

[86] SuperCDMS collaboration, R. Agnese et al., *Search for low-mass weakly interacting massive particles using voltage-assisted calorimetric ionization detection in the SuperCDMS experiment*, *Phys. Rev. Lett.* **112** (2014) 041302 [`arXiv:1309.3259`] [INSPIRE].

[87] XENON100 collaboration, E. Aprile et al., *Dark matter results from* 100 *live days of XENON100 data*, *Phys. Rev. Lett.* **107** (2011) 131302 [`arXiv:1104.2549`] [INSPIRE].

[88] LUX collaboration, D.S. Akerib et al., *First results from the LUX dark matter experiment at the Sanford Underground Research Facility*, *Phys. Rev. Lett.* **112** (2014) 091303 [`arXiv:1310.8214`] [INSPIRE].

[89] CRESST-II collaboration, G. Angloher et al., *Results on low mass WIMPs using an upgraded CRESST-II detector*, *Eur. Phys. J.* **C 74** (2014) 3184 [`arXiv:1407.3146`] [INSPIRE].

[90] CRESST collaboration, G. Angloher et al., *Results on light dark matter particles with a low-threshold CRESST-II detector*, *Eur. Phys. J.* **C 76** (2016) 25 [`arXiv:1509.01515`] [INSPIRE].

[91] T. Lin, E.W. Kolb and L.-T. Wang, *Probing dark matter couplings to top and bottom quarks at the LHC*, *Phys. Rev.* **D 88** (2013) 063510 [`arXiv:1303.6638`] [INSPIRE].

The CMS collaboration

Yerevan Physics Institute, Yerevan, Armenia
V. Khachatryan, A.M. Sirunyan, A. Tumasyan

Institut für Hochenergiephysik der OeAW, Wien, Austria
W. Adam, E. Asilar, T. Bergauer, J. Brandstetter, E. Brondolin, M. Dragicevic, J. Erö, M. Flechl, M. Friedl, R. Frühwirth[1], V.M. Ghete, C. Hartl, N. Hörmann, J. Hrubec, M. Jeitler[1], A. König, M. Krammer[1], I. Krätschmer, D. Liko, T. Matsushita, I. Mikulec, D. Rabady, N. Rad, B. Rahbaran, H. Rohringer, J. Schieck[1], R. Schöfbeck, J. Strauss, W. Treberer-Treberspurg, W. Waltenberger, C.-E. Wulz[1]

National Centre for Particle and High Energy Physics, Minsk, Belarus
V. Mossolov, N. Shumeiko, J. Suarez Gonzalez

Universiteit Antwerpen, Antwerpen, Belgium
S. Alderweireldt, T. Cornelis, E.A. De Wolf, X. Janssen, A. Knutsson, J. Lauwers, S. Luyckx, M. Van De Klundert, H. Van Haevermaet, P. Van Mechelen, N. Van Remortel, A. Van Spilbeeck

Vrije Universiteit Brussel, Brussel, Belgium
S. Abu Zeid, F. Blekman, J. D'Hondt, N. Daci, I. De Bruyn, K. Deroover, N. Heracleous, J. Keaveney, S. Lowette, S. Moortgat, L. Moreels, A. Olbrechts, Q. Python, D. Strom, S. Tavernier, W. Van Doninck, P. Van Mulders, G.P. Van Onsem, I. Van Parijs

Université Libre de Bruxelles, Bruxelles, Belgium
P. Barria, H. Brun, C. Caillol, B. Clerbaux, G. De Lentdecker, G. Fasanella, L. Favart, R. Goldouzian, A. Grebenyuk, G. Karapostoli, T. Lenzi, A. Léonard, T. Maerschalk, A. Marinov, L. Perniè, A. Randle-conde, T. Seva, C. Vander Velde, P. Vanlaer, R. Yonamine, F. Zenoni, F. Zhang[2]

Ghent University, Ghent, Belgium
K. Beernaert, L. Benucci, A. Cimmino, S. Crucy, D. Dobur, A. Fagot, G. Garcia, M. Gul, J. Mccartin, A.A. Ocampo Rios, D. Poyraz, D. Ryckbosch, S. Salva, M. Sigamani, M. Tytgat, W. Van Driessche, E. Yazgan, N. Zaganidis

Université Catholique de Louvain, Louvain-la-Neuve, Belgium
S. Basegmez, C. Beluffi[3], O. Bondu, S. Brochet, G. Bruno, A. Caudron, L. Ceard, S. De Visscher, C. Delaere, M. Delcourt, D. Favart, L. Forthomme, A. Giammanco, A. Jafari, P. Jez, M. Komm, V. Lemaitre, A. Mertens, M. Musich, C. Nuttens, L. Perrini, K. Piotrzkowski, A. Popov[4], L. Quertenmont, M. Selvaggi, M. Vidal Marono

Université de Mons, Mons, Belgium
N. Beliy, G.H. Hammad

Centro Brasileiro de Pesquisas Fisicas, Rio de Janeiro, Brazil
W.L. Aldá Júnior, F.L. Alves, G.A. Alves, L. Brito, M. Correa Martins Junior, M. Hamer, C. Hensel, A. Moraes, M.E. Pol, P. Rebello Teles

Universidade do Estado do Rio de Janeiro, Rio de Janeiro, Brazil

E. Belchior Batista Das Chagas, W. Carvalho, J. Chinellato[5], A. Custódio, E.M. Da Costa, D. De Jesus Damiao, C. De Oliveira Martins, S. Fonseca De Souza, L.M. Huertas Guativa, H. Malbouisson, D. Matos Figueiredo, C. Mora Herrera, L. Mundim, H. Nogima, W.L. Prado Da Silva, A. Santoro, A. Sznajder, E.J. Tonelli Manganote[5], A. Vilela Pereira

Universidade Estadual Paulista [a], Universidade Federal do ABC [b], São Paulo, Brazil

S. Ahuja[a], C.A. Bernardes[b], A. De Souza Santos[b], S. Dogra[a], T.R. Fernandez Perez Tomei[a], E.M. Gregores[b], P.G. Mercadante[b], C.S. Moon[a,6], S.F. Novaes[a], Sandra S. Padula[a], D. Romero Abad[b], J.C. Ruiz Vargas

Institute for Nuclear Research and Nuclear Energy, Sofia, Bulgaria

A. Aleksandrov, R. Hadjiiska, P. Iaydjiev, M. Rodozov, S. Stoykova, G. Sultanov, M. Vutova

University of Sofia, Sofia, Bulgaria

A. Dimitrov, I. Glushkov, L. Litov, B. Pavlov, P. Petkov

Beihang University, Beijing, China

W. Fang[7]

Institute of High Energy Physics, Beijing, China

M. Ahmad, J.G. Bian, G.M. Chen, H.S. Chen, M. Chen, T. Cheng, R. Du, C.H. Jiang, D. Leggat, R. Plestina[8], F. Romeo, S.M. Shaheen, A. Spiezia, J. Tao, C. Wang, Z. Wang, H. Zhang

State Key Laboratory of Nuclear Physics and Technology, Peking University, Beijing, China

C. Asawatangtrakuldee, Y. Ban, Q. Li, S. Liu, Y. Mao, S.J. Qian, D. Wang, Z. Xu

Universidad de Los Andes, Bogota, Colombia

C. Avila, A. Cabrera, L.F. Chaparro Sierra, C. Florez, J.P. Gomez, B. Gomez Moreno, J.C. Sanabria

University of Split, Faculty of Electrical Engineering, Mechanical Engineering and Naval Architecture, Split, Croatia

N. Godinovic, D. Lelas, I. Puljak, P.M. Ribeiro Cipriano

University of Split, Faculty of Science, Split, Croatia

Z. Antunovic, M. Kovac

Institute Rudjer Boskovic, Zagreb, Croatia

V. Brigljevic, K. Kadija, J. Luetic, S. Micanovic, L. Sudic

University of Cyprus, Nicosia, Cyprus

A. Attikis, G. Mavromanolakis, J. Mousa, C. Nicolaou, F. Ptochos, P.A. Razis, H. Rykaczewski

Charles University, Prague, Czech Republic
M. Finger[9], M. Finger Jr.[9]

Academy of Scientific Research and Technology of the Arab Republic of Egypt, Egyptian Network of High Energy Physics, Cairo, Egypt
A. Awad, E. El-khateeb[10,10], S. Elgammal[11], A. Mohamed[12]

National Institute of Chemical Physics and Biophysics, Tallinn, Estonia
B. Calpas, M. Kadastik, M. Murumaa, M. Raidal, A. Tiko, C. Veelken

Department of Physics, University of Helsinki, Helsinki, Finland
P. Eerola, J. Pekkanen, M. Voutilainen

Helsinki Institute of Physics, Helsinki, Finland
J. Härkönen, V. Karimäki, R. Kinnunen, T. Lampén, K. Lassila-Perini, S. Lehti, T. Lindén, P. Luukka, T. Peltola, J. Tuominiemi, E. Tuovinen, L. Wendland

Lappeenranta University of Technology, Lappeenranta, Finland
J. Talvitie, T. Tuuva

DSM/IRFU, CEA/Saclay, Gif-sur-Yvette, France
M. Besancon, F. Couderc, M. Dejardin, D. Denegri, B. Fabbro, J.L. Faure, C. Favaro, F. Ferri, S. Ganjour, A. Givernaud, P. Gras, G. Hamel de Monchenault, P. Jarry, E. Locci, M. Machet, J. Malcles, J. Rander, A. Rosowsky, M. Titov, A. Zghiche

Laboratoire Leprince-Ringuet, Ecole Polytechnique, IN2P3-CNRS, Palaiseau, France
A. Abdulsalam, I. Antropov, S. Baffioni, F. Beaudette, P. Busson, L. Cadamuro, E. Chapon, C. Charlot, O. Davignon, N. Filipovic, R. Granier de Cassagnac, M. Jo, S. Lisniak, L. Mastrolorenzo, P. Miné, I.N. Naranjo, M. Nguyen, C. Ochando, G. Ortona, P. Paganini, P. Pigard, S. Regnard, R. Salerno, J.B. Sauvan, Y. Sirois, T. Strebler, Y. Yilmaz, A. Zabi

Institut Pluridisciplinaire Hubert Curien, Université de Strasbourg, Université de Haute Alsace Mulhouse, CNRS/IN2P3, Strasbourg, France
J.-L. Agram[13], J. Andrea, A. Aubin, D. Bloch, J.-M. Brom, M. Buttignol, E.C. Chabert, N. Chanon, C. Collard, E. Conte[13], X. Coubez, J.-C. Fontaine[13], D. Gelé, U. Goerlach, C. Goetzmann, A.-C. Le Bihan, J.A. Merlin[14], K. Skovpen, P. Van Hove

Centre de Calcul de l'Institut National de Physique Nucleaire et de Physique des Particules, CNRS/IN2P3, Villeurbanne, France
S. Gadrat

Université de Lyon, Université Claude Bernard Lyon 1, CNRS-IN2P3, Institut de Physique Nucléaire de Lyon, Villeurbanne, France
S. Beauceron, C. Bernet, G. Boudoul, E. Bouvier, C.A. Carrillo Montoya, R. Chierici, D. Contardo, B. Courbon, P. Depasse, H. El Mamouni, J. Fan, J. Fay, S. Gascon, M. Gouzevitch, B. Ille, F. Lagarde, I.B. Laktineh, M. Lethuillier, L. Mirabito, A.L. Pequegnot, S. Perries, J.D. Ruiz Alvarez, D. Sabes, V. Sordini, M. Vander Donckt, P. Verdier, S. Viret

Georgian Technical University, Tbilisi, Georgia
T. Toriashvili[15]

Tbilisi State University, Tbilisi, Georgia
Z. Tsamalaidze[9]

RWTH Aachen University, I. Physikalisches Institut, Aachen, Germany
C. Autermann, S. Beranek, L. Feld, A. Heister, M.K. Kiesel, K. Klein, M. Lipinski, A. Ostapchuk, M. Preuten, F. Raupach, S. Schael, J.F. Schulte, T. Verlage, H. Weber, V. Zhukov[4]

RWTH Aachen University, III. Physikalisches Institut A, Aachen, Germany
M. Ata, M. Brodski, E. Dietz-Laursonn, D. Duchardt, M. Endres, M. Erdmann, S. Erdweg, T. Esch, R. Fischer, A. Güth, T. Hebbeker, C. Heidemann, K. Hoepfner, S. Knutzen, M. Merschmeyer, A. Meyer, P. Millet, S. Mukherjee, M. Olschewski, K. Padeken, P. Papacz, T. Pook, M. Radziej, H. Reithler, M. Rieger, F. Scheuch, L. Sonnenschein, D. Teyssier, S. Thüer

RWTH Aachen University, III. Physikalisches Institut B, Aachen, Germany
V. Cherepanov, Y. Erdogan, G. Flügge, H. Geenen, M. Geisler, F. Hoehle, B. Kargoll, T. Kress, A. Künsken, J. Lingemann, A. Nehrkorn, A. Nowack, I.M. Nugent, C. Pistone, O. Pooth, A. Stahl[14]

Deutsches Elektronen-Synchrotron, Hamburg, Germany
M. Aldaya Martin, I. Asin, N. Bartosik, O. Behnke, U. Behrens, K. Borras[16], A. Burgmeier, A. Campbell, C. Contreras-Campana, F. Costanza, C. Diez Pardos, G. Dolinska, S. Dooling, T. Dorland, G. Eckerlin, D. Eckstein, T. Eichhorn, G. Flucke, E. Gallo[17], J. Garay Garcia, A. Geiser, A. Gizhko, P. Gunnellini, J. Hauk, M. Hempel[18], H. Jung, A. Kalogeropoulos, O. Karacheban[18], M. Kasemann, P. Katsas, J. Kieseler, C. Kleinwort, I. Korol, W. Lange, J. Leonard, K. Lipka, A. Lobanov, W. Lohmann[18], R. Mankel, I.-A. Melzer-Pellmann, A.B. Meyer, G. Mittag, J. Mnich, A. Mussgiller, S. Naumann-Emme, A. Nayak, E. Ntomari, H. Perrey, D. Pitzl, R. Placakyte, A. Raspereza, B. Roland, M.Ö. Sahin, P. Saxena, T. Schoerner-Sadenius, C. Seitz, S. Spannagel, N. Stefaniuk, K.D. Trippkewitz, R. Walsh, C. Wissing

University of Hamburg, Hamburg, Germany
V. Blobel, M. Centis Vignali, A.R. Draeger, T. Dreyer, J. Erfle, E. Garutti, K. Goebel, D. Gonzalez, M. Görner, J. Haller, M. Hoffmann, R.S. Höing, A. Junkes, R. Klanner, R. Kogler, N. Kovalchuk, T. Lapsien, T. Lenz, I. Marchesini, D. Marconi, M. Meyer, M. Niedziela, D. Nowatschin, J. Ott, F. Pantaleo[14], T. Peiffer, A. Perieanu, N. Pietsch, J. Poehlsen, C. Sander, C. Scharf, P. Schleper, E. Schlieckau, A. Schmidt, S. Schumann, J. Schwandt, V. Sola, H. Stadie, G. Steinbrück, F.M. Stober, H. Tholen, D. Troendle, E. Usai, L. Vanelderen, A. Vanhoefer, B. Vormwald

Institut für Experimentelle Kernphysik, Karlsruhe, Germany
C. Barth, C. Baus, J. Berger, C. Böser, E. Butz, T. Chwalek, F. Colombo, W. De Boer, A. Descroix, A. Dierlamm, S. Fink, F. Frensch, R. Friese, M. Giffels, A. Gilbert, D. Haitz,

F. Hartmann[14], S.M. Heindl, U. Husemann, I. Katkov[4], A. Kornmayer[14], P. Lobelle Pardo, B. Maier, H. Mildner, M.U. Mozer, T. Müller, Th. Müller, M. Plagge, G. Quast, K. Rabbertz, S. Röcker, F. Roscher, M. Schröder, G. Sieber, H.J. Simonis, R. Ulrich, J. Wagner-Kuhr, S. Wayand, M. Weber, T. Weiler, S. Williamson, C. Wöhrmann, R. Wolf

Institute of Nuclear and Particle Physics (INPP), NCSR Demokritos, Aghia Paraskevi, Greece

G. Anagnostou, G. Daskalakis, T. Geralis, V.A. Giakoumopoulou, A. Kyriakis, D. Loukas, A. Psallidas, I. Topsis-Giotis

National and Kapodistrian University of Athens, Athens, Greece

A. Agapitos, S. Kesisoglou, A. Panagiotou, N. Saoulidou, E. Tziaferi

University of Ioánnina, Ioánnina, Greece

I. Evangelou, G. Flouris, C. Foudas, P. Kokkas, N. Loukas, N. Manthos, I. Papadopoulos, E. Paradas, J. Strologas

Wigner Research Centre for Physics, Budapest, Hungary

G. Bencze, C. Hajdu, A. Hazi, P. Hidas, D. Horvath[19], F. Sikler, V. Veszpremi, G. Vesztergombi[20], A.J. Zsigmond

Institute of Nuclear Research ATOMKI, Debrecen, Hungary

N. Beni, S. Czellar, J. Karancsi[21], J. Molnar, Z. Szillasi[14]

University of Debrecen, Debrecen, Hungary

M. Bartók[20], A. Makovec, P. Raics, Z.L. Trocsanyi, B. Ujvari

National Institute of Science Education and Research, Bhubaneswar, India

S. Choudhury[22], P. Mal, K. Mandal, D.K. Sahoo, N. Sahoo, S.K. Swain

Panjab University, Chandigarh, India

S. Bansal, S.B. Beri, V. Bhatnagar, R. Chawla, R. Gupta, U.Bhawandeep, A.K. Kalsi, A. Kaur, M. Kaur, R. Kumar, A. Mehta, M. Mittal, J.B. Singh, G. Walia

University of Delhi, Delhi, India

Ashok Kumar, A. Bhardwaj, B.C. Choudhary, R.B. Garg, S. Malhotra, M. Naimuddin, N. Nishu, K. Ranjan, R. Sharma, V. Sharma

Saha Institute of Nuclear Physics, Kolkata, India

R. Bhattacharya, S. Bhattacharya, K. Chatterjee, S. Dey, S. Dutta, S. Ghosh, N. Majumdar, A. Modak, K. Mondal, S. Mukhopadhyay, S. Nandan, A. Purohit, A. Roy, D. Roy, S. Roy Chowdhury, S. Sarkar, M. Sharan

Bhabha Atomic Research Centre, Mumbai, India

R. Chudasama, D. Dutta, V. Jha, V. Kumar, A.K. Mohanty[14], L.M. Pant, P. Shukla, A. Topkar

Tata Institute of Fundamental Research, Mumbai, India

T. Aziz, S. Banerjee, S. Bhowmik[23], R.M. Chatterjee, R.K. Dewanjee, S. Dugad, S. Ganguly, S. Ghosh, M. Guchait, A. Gurtu[24], Sa. Jain, G. Kole, S. Kumar, B. Mahakud,

M. Maity[23], G. Majumder, K. Mazumdar, S. Mitra, G.B. Mohanty, B. Parida, T. Sarkar[23], N. Sur, B. Sutar, N. Wickramage[25]

Indian Institute of Science Education and Research (IISER), Pune, India

S. Chauhan, S. Dube, A. Kapoor, K. Kothekar, A. Rane, S. Sharma

Institute for Research in Fundamental Sciences (IPM), Tehran, Iran

H. Bakhshiansohi, H. Behnamian, S.M. Etesami[26], A. Fahim[27], M. Khakzad, M. Mohammadi Najafabadi, M. Naseri, S. Paktinat Mehdiabadi, F. Rezaei Hosseinabadi, B. Safarzadeh[28], M. Zeinali

University College Dublin, Dublin, Ireland

M. Felcini, M. Grunewald

INFN Sezione di Bari [a], Università di Bari [b], Politecnico di Bari [c], Bari, Italy

M. Abbrescia[a,b], C. Calabria[a,b], C. Caputo[a,b], A. Colaleo[a], D. Creanza[a,c], L. Cristella[a,b], N. De Filippis[a,c], M. De Palma[a,b], L. Fiore[a], G. Iaselli[a,c], G. Maggi[a,c], M. Maggi[a], G. Miniello[a,b], S. My[a,c], S. Nuzzo[a,b], A. Pompili[a,b], G. Pugliese[a,c], R. Radogna[a,b], A. Ranieri[a], G. Selvaggi[a,b], L. Silvestris[a,14], R. Venditti[a,b]

INFN Sezione di Bologna [a], Università di Bologna [b], Bologna, Italy

G. Abbiendi[a], C. Battilana[14], D. Bonacorsi[a,b], S. Braibant-Giacomelli[a,b], L. Brigliadori[a,b], R. Campanini[a,b], P. Capiluppi[a,b], A. Castro[a,b], F.R. Cavallo[a], S.S. Chhibra[a,b], G. Codispoti[a,b], M. Cuffiani[a,b], G.M. Dallavalle[a], F. Fabbri[a], A. Fanfani[a,b], D. Fasanella[a,b], P. Giacomelli[a], C. Grandi[a], L. Guiducci[a,b], S. Marcellini[a], G. Masetti[a], A. Montanari[a], F.L. Navarria[a,b], A. Perrotta[a], A.M. Rossi[a,b], T. Rovelli[a,b], G.P. Siroli[a,b], N. Tosi[a,b,14]

INFN Sezione di Catania [a], Università di Catania [b], Catania, Italy

G. Cappello[b], M. Chiorboli[a,b], S. Costa[a,b], A. Di Mattia[a], F. Giordano[a,b], R. Potenza[a,b], A. Tricomi[a,b], C. Tuve[a,b]

INFN Sezione di Firenze [a], Università di Firenze [b], Firenze, Italy

G. Barbagli[a], V. Ciulli[a,b], C. Civinini[a], R. D'Alessandro[a,b], E. Focardi[a,b], V. Gori[a,b], P. Lenzi[a,b], M. Meschini[a], S. Paoletti[a], G. Sguazzoni[a], L. Viliani[a,b,14]

INFN Laboratori Nazionali di Frascati, Frascati, Italy

L. Benussi, S. Bianco, F. Fabbri, D. Piccolo, F. Primavera[14]

INFN Sezione di Genova [a], Università di Genova [b], Genova, Italy

V. Calvelli[a,b], F. Ferro[a], M. Lo Vetere[a,b], M.R. Monge[a,b], E. Robutti[a], S. Tosi[a,b]

INFN Sezione di Milano-Bicocca [a], Università di Milano-Bicocca [b], Milano, Italy

L. Brianza, M.E. Dinardo[a,b], S. Fiorendi[a,b], S. Gennai[a], R. Gerosa[a,b], A. Ghezzi[a,b], P. Govoni[a,b], S. Malvezzi[a], R.A. Manzoni[a,b,14], B. Marzocchi[a,b], D. Menasce[a], L. Moroni[a], M. Paganoni[a,b], D. Pedrini[a], S. Ragazzi[a,b], N. Redaelli[a], T. Tabarelli de Fatis[a,b]

INFN Sezione di Napoli [a], Università di Napoli 'Federico II' [b], Napoli, Italy, Università della Basilicata [c], Potenza, Italy, Università G. Marconi [d], Roma, Italy

S. Buontempo[a], N. Cavallo[a,c], S. Di Guida[a,d,14], M. Esposito[a,b], F. Fabozzi[a,c], A.O.M. Iorio[a,b], G. Lanza[a], L. Lista[a], S. Meola[a,d,14], M. Merola[a], P. Paolucci[a,14], C. Sciacca[a,b], F. Thyssen

INFN Sezione di Padova [a], Università di Padova [b], Padova, Italy, Università di Trento [c], Trento, Italy

P. Azzi[a,14], N. Bacchetta[a], L. Benato[a,b], D. Bisello[a,b], A. Boletti[a,b], R. Carlin[a,b], P. Checchia[a], M. Dall'Osso[a,b,14], T. Dorigo[a], U. Dosselli[a], F. Gasparini[a,b], U. Gasparini[a,b], A. Gozzelino[a], S. Lacaprara[a], M. Margoni[a,b], A.T. Meneguzzo[a,b], F. Montecassiano[a], M. Passaseo[a], J. Pazzini[a,b,14], M. Pegoraro[a], N. Pozzobon[a,b], P. Ronchese[a,b], F. Simonetto[a,b], E. Torassa[a], M. Tosi[a,b], M. Zanetti, P. Zotto[a,b], A. Zucchetta[a,b,14], G. Zumerle[a,b]

INFN Sezione di Pavia [a], Università di Pavia [b], Pavia, Italy

A. Braghieri[a], A. Magnani[a,b], P. Montagna[a,b], S.P. Ratti[a,b], V. Re[a], C. Riccardi[a,b], P. Salvini[a], I. Vai[a,b], P. Vitulo[a,b]

INFN Sezione di Perugia [a], Università di Perugia [b], Perugia, Italy

L. Alunni Solestizi[a,b], G.M. Bilei[a], D. Ciangottini[a,b], L. Fanò[a,b], P. Lariccia[a,b], G. Mantovani[a,b], M. Menichelli[a], A. Saha[a], A. Santocchia[a,b]

INFN Sezione di Pisa [a], Università di Pisa [b], Scuola Normale Superiore di Pisa [c], Pisa, Italy

K. Androsov[a,29], P. Azzurri[a,14], G. Bagliesi[a], J. Bernardini[a], T. Boccali[a], R. Castaldi[a], M.A. Ciocci[a,29], R. Dell'Orso[a], S. Donato[a,c], G. Fedi, L. Foà[a,c†], A. Giassi[a], M.T. Grippo[a,29], F. Ligabue[a,c], T. Lomtadze[a], L. Martini[a,b], A. Messineo[a,b], F. Palla[a], A. Rizzi[a,b], A. Savoy-Navarro[a,30], P. Spagnolo[a], R. Tenchini[a], G. Tonelli[a,b], A. Venturi[a], P.G. Verdini[a]

INFN Sezione di Roma [a], Università di Roma [b], Roma, Italy

L. Barone[a,b], F. Cavallari[a], G. D'imperio[a,b,14], D. Del Re[a,b,14], M. Diemoz[a], S. Gelli[a,b], C. Jorda[a], E. Longo[a,b], F. Margaroli[a,b], P. Meridiani[a], G. Organtini[a,b], R. Paramatti[a], F. Preiato[a,b], S. Rahatlou[a,b], C. Rovelli[a], F. Santanastasio[a,b]

INFN Sezione di Torino [a], Università di Torino [b], Torino, Italy, Università del Piemonte Orientale [c], Novara, Italy

N. Amapane[a,b], R. Arcidiacono[a,c,14], S. Argiro[a,b], M. Arneodo[a,c], R. Bellan[a,b], C. Biino[a], N. Cartiglia[a], M. Costa[a,b], R. Covarelli[a,b], A. Degano[a,b], N. Demaria[a], L. Finco[a,b], B. Kiani[a,b], C. Mariotti[a], S. Maselli[a], E. Migliore[a,b], V. Monaco[a,b], E. Monteil[a,b], M.M. Obertino[a,b], L. Pacher[a,b], N. Pastrone[a], M. Pelliccioni[a], G.L. Pinna Angioni[a,b], F. Ravera[a,b], A. Romero[a,b], M. Ruspa[a,c], R. Sacchi[a,b], A. Solano[a,b], A. Staiano[a]

INFN Sezione di Trieste [a], Università di Trieste [b], Trieste, Italy

S. Belforte[a], V. Candelise[a,b], M. Casarsa[a], F. Cossutti[a], G. Della Ricca[a,b], B. Gobbo[a], C. La Licata[a,b], A. Schizzi[a,b], A. Zanetti[a]

Kangwon National University, Chunchon, Korea

A. Kropivnitskaya, S.K. Nam

Kyungpook National University, Daegu, Korea

D.H. Kim, G.N. Kim, M.S. Kim, D.J. Kong, S. Lee, S.W. Lee, Y.D. Oh, A. Sakharov, D.C. Son

Chonbuk National University, Jeonju, Korea

J.A. Brochero Cifuentes, H. Kim, T.J. Kim[31]

Chonnam National University, Institute for Universe and Elementary Particles, Kwangju, Korea

S. Song

Korea University, Seoul, Korea

S. Cho, S. Choi, Y. Go, D. Gyun, B. Hong, H. Kim, Y. Kim, B. Lee, K. Lee, K.S. Lee, S. Lee, J. Lim, S.K. Park, Y. Roh

Seoul National University, Seoul, Korea

H.D. Yoo

University of Seoul, Seoul, Korea

M. Choi, H. Kim, J.H. Kim, J.S.H. Lee, I.C. Park, G. Ryu, M.S. Ryu

Sungkyunkwan University, Suwon, Korea

Y. Choi, J. Goh, D. Kim, E. Kwon, J. Lee, I. Yu

Vilnius University, Vilnius, Lithuania

V. Dudenas, A. Juodagalvis, J. Vaitkus

National Centre for Particle Physics, Universiti Malaya, Kuala Lumpur, Malaysia

I. Ahmed, Z.A. Ibrahim, J.R. Komaragiri, M.A.B. Md Ali[32], F. Mohamad Idris[33], W.A.T. Wan Abdullah, M.N. Yusli, Z. Zolkapli

Centro de Investigacion y de Estudios Avanzados del IPN, Mexico City, Mexico

E. Casimiro Linares, H. Castilla-Valdez, E. De La Cruz-Burelo, I. Heredia-De La Cruz[34], A. Hernandez-Almada, R. Lopez-Fernandez, J. Mejia Guisao, A. Sanchez-Hernandez

Universidad Iberoamericana, Mexico City, Mexico

S. Carrillo Moreno, F. Vazquez Valencia

Benemerita Universidad Autonoma de Puebla, Puebla, Mexico

I. Pedraza, H.A. Salazar Ibarguen

Universidad Autónoma de San Luis Potosí, San Luis Potosí, Mexico

A. Morelos Pineda

University of Auckland, Auckland, New Zealand
D. Krofcheck

University of Canterbury, Christchurch, New Zealand
P.H. Butler

National Centre for Physics, Quaid-I-Azam University, Islamabad, Pakistan
A. Ahmad, M. Ahmad, Q. Hassan, H.R. Hoorani, W.A. Khan, T. Khurshid, M. Shoaib, M. Waqas

National Centre for Nuclear Research, Swierk, Poland
H. Bialkowska, M. Bluj, B. Boimska, T. Frueboes, M. Górski, M. Kazana, K. Nawrocki, K. Romanowska-Rybinska, M. Szleper, P. Traczyk, P. Zalewski

Institute of Experimental Physics, Faculty of Physics, University of Warsaw, Warsaw, Poland
G. Brona, K. Bunkowski, A. Byszuk[35], K. Doroba, A. Kalinowski, M. Konecki, J. Krolikowski, M. Misiura, M. Olszewski, M. Walczak

Laboratório de Instrumentação e Física Experimental de Partículas, Lisboa, Portugal
P. Bargassa, C. Beirão Da Cruz E Silva, A. Di Francesco, P. Faccioli, P.G. Ferreira Parracho, M. Gallinaro, J. Hollar, N. Leonardo, L. Lloret Iglesias, M.V. Nemallapudi, F. Nguyen, J. Rodrigues Antunes, J. Seixas, O. Toldaiev, D. Vadruccio, J. Varela, P. Vischia

Joint Institute for Nuclear Research, Dubna, Russia
I. Golutvin, N. Gorbounov, I. Gorbunov, V. Karjavin, G. Kozlov, A. Lanev, A. Malakhov, V. Matveev[36,37], P. Moisenz, V. Palichik, V. Perelygin, M. Savina, S. Shmatov, S. Shulha, N. Skatchkov, V. Smirnov, E. Tikhonenko, A. Zarubin

Petersburg Nuclear Physics Institute, Gatchina (St. Petersburg), Russia
V. Golovtsov, Y. Ivanov, V. Kim[38], E. Kuznetsova, P. Levchenko, V. Murzin, V. Oreshkin, I. Smirnov, V. Sulimov, L. Uvarov, S. Vavilov, A. Vorobyev

Institute for Nuclear Research, Moscow, Russia
Yu. Andreev, A. Dermenev, S. Gninenko, N. Golubev, A. Karneyeu, M. Kirsanov, N. Krasnikov, A. Pashenkov, D. Tlisov, A. Toropin

Institute for Theoretical and Experimental Physics, Moscow, Russia
V. Epshteyn, V. Gavrilov, N. Lychkovskaya, V. Popov, I. Pozdnyakov, G. Safronov, A. Spiridonov, E. Vlasov, A. Zhokin

National Research Nuclear University 'Moscow Engineering Physics Institute' (MEPhI), Moscow, Russia
R. Chistov, M. Danilov, O. Markin, V. Rusinov, E. Tarkovskii

P.N. Lebedev Physical Institute, Moscow, Russia
V. Andreev, M. Azarkin[37], I. Dremin[37], M. Kirakosyan, A. Leonidov[37], G. Mesyats, S.V. Rusakov

Skobeltsyn Institute of Nuclear Physics, Lomonosov Moscow State University, Moscow, Russia

A. Baskakov, A. Belyaev, E. Boos, M. Dubinin[39], L. Dudko, A. Ershov, A. Gribushin, V. Klyukhin, O. Kodolova, I. Lokhtin, I. Miagkov, S. Obraztsov, S. Petrushanko, V. Savrin, A. Snigirev

State Research Center of Russian Federation, Institute for High Energy Physics, Protvino, Russia

I. Azhgirey, I. Bayshev, S. Bitioukov, V. Kachanov, A. Kalinin, D. Konstantinov, V. Krychkine, V. Petrov, R. Ryutin, A. Sobol, L. Tourtchanovitch, S. Troshin, N. Tyurin, A. Uzunian, A. Volkov

University of Belgrade, Faculty of Physics and Vinca Institute of Nuclear Sciences, Belgrade, Serbia

P. Adzic[40], P. Cirkovic, D. Devetak, J. Milosevic, V. Rekovic

Centro de Investigaciones Energéticas Medioambientales y Tecnológicas (CIEMAT), Madrid, Spain

J. Alcaraz Maestre, E. Calvo, M. Cerrada, M. Chamizo Llatas, N. Colino, B. De La Cruz, A. Delgado Peris, A. Escalante Del Valle, C. Fernandez Bedoya, J.P. Fernández Ramos, J. Flix, M.C. Fouz, P. Garcia-Abia, O. Gonzalez Lopez, S. Goy Lopez, J.M. Hernandez, M.I. Josa, E. Navarro De Martino, A. Pérez-Calero Yzquierdo, J. Puerta Pelayo, A. Quintario Olmeda, I. Redondo, L. Romero, M.S. Soares

Universidad Autónoma de Madrid, Madrid, Spain

J.F. de Trocóniz, M. Missiroli, D. Moran

Universidad de Oviedo, Oviedo, Spain

J. Cuevas, J. Fernandez Menendez, S. Folgueras, I. Gonzalez Caballero, E. Palencia Cortezon[14], J.M. Vizan Garcia

Instituto de Física de Cantabria (IFCA), CSIC-Universidad de Cantabria, Santander, Spain

I.J. Cabrillo, A. Calderon, J.R. Castiñeiras De Saa, E. Curras, P. De Castro Manzano, M. Fernandez, J. Garcia-Ferrero, G. Gomez, A. Lopez Virto, J. Marco, R. Marco, C. Martinez Rivero, F. Matorras, J. Piedra Gomez, T. Rodrigo, A.Y. Rodríguez-Marrero, A. Ruiz-Jimeno, L. Scodellaro, N. Trevisani, I. Vila, R. Vilar Cortabitarte

CERN, European Organization for Nuclear Research, Geneva, Switzerland

D. Abbaneo, E. Auffray, G. Auzinger, M. Bachtis, P. Baillon, A.H. Ball, D. Barney, A. Benaglia, L. Benhabib, G.M. Berruti, P. Bloch, A. Bocci, A. Bonato, C. Botta, H. Breuker, T. Camporesi, R. Castello, M. Cepeda, G. Cerminara, M. D'Alfonso, D. d'Enterria, A. Dabrowski, V. Daponte, A. David, M. De Gruttola, F. De Guio, A. De Roeck, E. Di Marco[41], M. Dobson, M. Dordevic, B. Dorney, T. du Pree, D. Duggan, M. Dünser, N. Dupont, A. Elliott-Peisert, G. Franzoni, J. Fulcher, W. Funk, D. Gigi, K. Gill, D. Giordano, M. Girone, F. Glege, R. Guida, S. Gundacker, M. Guthoff, J. Hammer, P. Harris, J. Hegeman, V. Innocente, P. Janot, H. Kirschenmann, V. Knünz, M.J. Kortelainen,

K. Kousouris, P. Lecoq, C. Lourenço, M.T. Lucchini, N. Magini, L. Malgeri, M. Mannelli, A. Martelli, L. Masetti, F. Meijers, S. Mersi, E. Meschi, F. Moortgat, S. Morovic, M. Mulders, H. Neugebauer, S. Orfanelli[42], L. Orsini, L. Pape, E. Perez, M. Peruzzi, A. Petrilli, G. Petrucciani, A. Pfeiffer, M. Pierini, D. Piparo, A. Racz, T. Reis, G. Rolandi[43], M. Rovere, M. Ruan, H. Sakulin, C. Schäfer, C. Schwick, M. Seidel, A. Sharma, P. Silva, M. Simon, P. Sphicas[44], J. Steggemann, M. Stoye, Y. Takahashi, D. Treille, A. Triossi, A. Tsirou, G.I. Veres[20], N. Wardle, H.K. Wöhri, A. Zagozdzinska[35], W.D. Zeuner

Paul Scherrer Institut, Villigen, Switzerland

W. Bertl, K. Deiters, W. Erdmann, R. Horisberger, Q. Ingram, H.C. Kaestli, D. Kotlinski, U. Langenegger, T. Rohe

Institute for Particle Physics, ETH Zurich, Zurich, Switzerland

F. Bachmair, L. Bäni, L. Bianchini, B. Casal, G. Dissertori, M. Dittmar, M. Donegà, P. Eller, C. Grab, C. Heidegger, D. Hits, J. Hoss, G. Kasieczka, P. Lecomte[†], W. Lustermann, B. Mangano, M. Marionneau, P. Martinez Ruiz del Arbol, M. Masciovecchio, M.T. Meinhard, D. Meister, F. Micheli, P. Musella, F. Nessi-Tedaldi, F. Pandolfi, J. Pata, F. Pauss, G. Perrin, L. Perrozzi, M. Quittnat, M. Rossini, M. Schönenberger, A. Starodumov[45], M. Takahashi, V.R. Tavolaro, K. Theofilatos, R. Wallny

Universität Zürich, Zurich, Switzerland

T.K. Aarrestad, C. Amsler[46], L. Caminada, M.F. Canelli, V. Chiochia, A. De Cosa, C. Galloni, A. Hinzmann, T. Hreus, B. Kilminster, C. Lange, J. Ngadiuba, D. Pinna, G. Rauco, P. Robmann, D. Salerno, Y. Yang

National Central University, Chung-Li, Taiwan

K.H. Chen, T.H. Doan, Sh. Jain, R. Khurana, M. Konyushikhin, C.M. Kuo, W. Lin, Y.J. Lu, A. Pozdnyakov, S.S. Yu

National Taiwan University (NTU), Taipei, Taiwan

Arun Kumar, P. Chang, Y.H. Chang, Y.W. Chang, Y. Chao, K.F. Chen, P.H. Chen, C. Dietz, F. Fiori, U. Grundler, W.-S. Hou, Y. Hsiung, Y.F. Liu, R.-S. Lu, M. Miñano Moya, E. Petrakou, J.f. Tsai, Y.M. Tzeng

Chulalongkorn University, Faculty of Science, Department of Physics, Bangkok, Thailand

B. Asavapibhop, K. Kovitanggoon, G. Singh, N. Srimanobhas, N. Suwonjandee

Cukurova University, Adana, Turkey

A. Adiguzel, M.N. Bakirci[47], S. Cerci[48], S. Damarseckin, Z.S. Demiroglu, C. Dozen, I. Dumanoglu, E. Eskut, S. Girgis, G. Gokbulut, Y. Guler, E. Gurpinar, I. Hos, E.E. Kangal[49], G. Onengut[50], K. Ozdemir[51], A. Polatoz, D. Sunar Cerci[48], C. Zorbilmez

Middle East Technical University, Physics Department, Ankara, Turkey

B. Bilin, S. Bilmis, B. Isildak[52], G. Karapinar[53], M. Yalvac, M. Zeyrek

Bogazici University, Istanbul, Turkey

E. Gülmez, M. Kaya[54], O. Kaya[55], E.A. Yetkin[56], T. Yetkin[57]

Istanbul Technical University, Istanbul, Turkey
A. Cakir, K. Cankocak, S. Sen[58], F.I. Vardarlı

Institute for Scintillation Materials of National Academy of Science of Ukraine, Kharkov, Ukraine
B. Grynyov

National Scientific Center, Kharkov Institute of Physics and Technology, Kharkov, Ukraine
L. Levchuk, P. Sorokin

University of Bristol, Bristol, U.K.
R. Aggleton, F. Ball, L. Beck, J.J. Brooke, D. Burns, E. Clement, D. Cussans, H. Flacher, J. Goldstein, M. Grimes, G.P. Heath, H.F. Heath, J. Jacob, L. Kreczko, C. Lucas, Z. Meng, D.M. Newbold[59], S. Paramesvaran, A. Poll, T. Sakuma, S. Seif El Nasr-storey, S. Senkin, D. Smith, V.J. Smith

Rutherford Appleton Laboratory, Didcot, U.K.
K.W. Bell, A. Belyaev[60], C. Brew, R.M. Brown, L. Calligaris, D. Cieri, D.J.A. Cockerill, J.A. Coughlan, K. Harder, S. Harper, E. Olaiya, D. Petyt, C.H. Shepherd-Themistocleous, A. Thea, I.R. Tomalin, T. Williams, S.D. Worm

Imperial College, London, U.K.
M. Baber, R. Bainbridge, O. Buchmuller, A. Bundock, D. Burton, S. Casasso, M. Citron, D. Colling, L. Corpe, P. Dauncey, G. Davies, A. De Wit, M. Della Negra, P. Dunne, A. Elwood, D. Futyan, G. Hall, G. Iles, R. Lane, R. Lucas[59], L. Lyons, A.-M. Magnan, S. Malik, J. Nash, A. Nikitenko[45], J. Pela, B. Penning, M. Pesaresi, D.M. Raymond, A. Richards, A. Rose, C. Seez, A. Tapper, K. Uchida, M. Vazquez Acosta[61], T. Virdee, S.C. Zenz

Brunel University, Uxbridge, U.K.
J.E. Cole, P.R. Hobson, A. Khan, P. Kyberd, D. Leslie, I.D. Reid, P. Symonds, L. Teodorescu, M. Turner

Baylor University, Waco, U.S.A.
A. Borzou, K. Call, J. Dittmann, K. Hatakeyama, H. Liu, N. Pastika

The University of Alabama, Tuscaloosa, U.S.A.
O. Charaf, S.I. Cooper, C. Henderson, P. Rumerio

Boston University, Boston, U.S.A.
D. Arcaro, A. Avetisyan, T. Bose, D. Gastler, D. Rankin, C. Richardson, J. Rohlf, L. Sulak, D. Zou

Brown University, Providence, U.S.A.
J. Alimena, G. Benelli, E. Berry, D. Cutts, A. Ferapontov, A. Garabedian, J. Hakala, U. Heintz, O. Jesus, E. Laird, G. Landsberg, Z. Mao, M. Narain, S. Piperov, S. Sagir, R. Syarif

University of California, Davis, Davis, U.S.A.

R. Breedon, G. Breto, M. Calderon De La Barca Sanchez, S. Chauhan, M. Chertok, J. Conway, R. Conway, P.T. Cox, R. Erbacher, G. Funk, M. Gardner, W. Ko, R. Lander, C. Mclean, M. Mulhearn, D. Pellett, J. Pilot, F. Ricci-Tam, S. Shalhout, J. Smith, M. Squires, D. Stolp, M. Tripathi, S. Wilbur, R. Yohay

University of California, Los Angeles, U.S.A.

R. Cousins, P. Everaerts, A. Florent, J. Hauser, M. Ignatenko, D. Saltzberg, E. Takasugi, V. Valuev, M. Weber

University of California, Riverside, Riverside, U.S.A.

K. Burt, R. Clare, J. Ellison, J.W. Gary, G. Hanson, J. Heilman, M. Ivova PANEVA, P. Jandir, E. Kennedy, F. Lacroix, O.R. Long, M. Malberti, M. Olmedo Negrete, A. Shrinivas, H. Wei, S. Wimpenny, B. R. Yates

University of California, San Diego, La Jolla, U.S.A.

J.G. Branson, G.B. Cerati, S. Cittolin, R.T. D'Agnolo, M. Derdzinski, A. Holzner, R. Kelley, D. Klein, J. Letts, I. Macneill, D. Olivito, S. Padhi, M. Pieri, M. Sani, V. Sharma, S. Simon, M. Tadel, A. Vartak, S. Wasserbaech[62], C. Welke, F. Würthwein, A. Yagil, G. Zevi Della Porta

University of California, Santa Barbara, Santa Barbara, U.S.A.

J. Bradmiller-Feld, C. Campagnari, A. Dishaw, V. Dutta, K. Flowers, M. Franco Sevilla, P. Geffert, C. George, F. Golf, L. Gouskos, J. Gran, J. Incandela, N. Mccoll, S.D. Mullin, J. Richman, D. Stuart, I. Suarez, C. West, J. Yoo

California Institute of Technology, Pasadena, U.S.A.

D. Anderson, A. Apresyan, J. Bendavid, A. Bornheim, J. Bunn, Y. Chen, J. Duarte, A. Mott, H.B. Newman, C. Pena, M. Spiropulu, J.R. Vlimant, S. Xie, R.Y. Zhu

Carnegie Mellon University, Pittsburgh, U.S.A.

M.B. Andrews, V. Azzolini, A. Calamba, B. Carlson, T. Ferguson, M. Paulini, J. Russ, M. Sun, H. Vogel, I. Vorobiev

University of Colorado Boulder, Boulder, U.S.A.

J.P. Cumalat, W.T. Ford, A. Gaz, F. Jensen, A. Johnson, M. Krohn, T. Mulholland, U. Nauenberg, K. Stenson, S.R. Wagner

Cornell University, Ithaca, U.S.A.

J. Alexander, A. Chatterjee, J. Chaves, J. Chu, S. Dittmer, N. Eggert, N. Mirman, G. Nicolas Kaufman, J.R. Patterson, A. Rinkevicius, A. Ryd, L. Skinnari, L. Soffi, W. Sun, S.M. Tan, W.D. Teo, J. Thom, J. Thompson, J. Tucker, Y. Weng, P. Wittich

Fermi National Accelerator Laboratory, Batavia, U.S.A.

S. Abdullin, M. Albrow, G. Apollinari, S. Banerjee, L.A.T. Bauerdick, A. Beretvas, J. Berryhill, P.C. Bhat, G. Bolla, K. Burkett, J.N. Butler, H.W.K. Cheung, F. Chlebana, S. Cihangir, V.D. Elvira, I. Fisk, J. Freeman, E. Gottschalk, L. Gray, D. Green, S. Grünendahl, O. Gutsche, J. Hanlon, D. Hare, R.M. Harris, S. Hasegawa, J. Hirschauer,

Z. Hu, B. Jayatilaka, S. Jindariani, M. Johnson, U. Joshi, B. Klima, B. Kreis, S. Lammel, J. Lewis, J. Linacre, D. Lincoln, R. Lipton, T. Liu, R. Lopes De Sá, J. Lykken, K. Maeshima, J.M. Marraffino, S. Maruyama, D. Mason, P. McBride, P. Merkel, S. Mrenna, S. Nahn, C. Newman-Holmes†, V. O'Dell, K. Pedro, O. Prokofyev, G. Rakness, E. Sexton-Kennedy, A. Soha, W.J. Spalding, L. Spiegel, S. Stoynev, N. Strobbe, L. Taylor, S. Tkaczyk, N.V. Tran, L. Uplegger, E.W. Vaandering, C. Vernieri, M. Verzocchi, R. Vidal, M. Wang, H.A. Weber, A. Whitbeck

University of Florida, Gainesville, U.S.A.

D. Acosta, P. Avery, P. Bortignon, D. Bourilkov, A. Brinkerhoff, A. Carnes, M. Carver, D. Curry, S. Das, R.D. Field, I.K. Furic, J. Konigsberg, A. Korytov, K. Kotov, P. Ma, K. Matchev, H. Mei, P. Milenovic[63], G. Mitselmakher, D. Rank, R. Rossin, L. Shchutska, M. Snowball, D. Sperka, N. Terentyev, L. Thomas, J. Wang, S. Wang, J. Yelton

Florida International University, Miami, U.S.A.

S. Linn, P. Markowitz, G. Martinez, J.L. Rodriguez

Florida State University, Tallahassee, U.S.A.

A. Ackert, J.R. Adams, T. Adams, A. Askew, S. Bein, J. Bochenek, B. Diamond, J. Haas, S. Hagopian, V. Hagopian, K.F. Johnson, A. Khatiwada, H. Prosper, M. Weinberg

Florida Institute of Technology, Melbourne, U.S.A.

M.M. Baarmand, V. Bhopatkar, S. Colafranceschi[64], M. Hohlmann, H. Kalakhety, D. Noonan, T. Roy, F. Yumiceva

University of Illinois at Chicago (UIC), Chicago, U.S.A.

M.R. Adams, L. Apanasevich, D. Berry, R.R. Betts, I. Bucinskaite, R. Cavanaugh, O. Evdokimov, L. Gauthier, C.E. Gerber, D.J. Hofman, P. Kurt, C. O'Brien, I.D. Sandoval Gonzalez, P. Turner, N. Varelas, Z. Wu, M. Zakaria, J. Zhang

The University of Iowa, Iowa City, U.S.A.

B. Bilki[65], W. Clarida, K. Dilsiz, S. Durgut, R.P. Gandrajula, M. Haytmyradov, V. Khristenko, J.-P. Merlo, H. Mermerkaya[66], A. Mestvirishvili, A. Moeller, J. Nachtman, H. Ogul, Y. Onel, F. Ozok[67], A. Penzo, C. Snyder, E. Tiras, J. Wetzel, K. Yi

Johns Hopkins University, Baltimore, U.S.A.

I. Anderson, B.A. Barnett, B. Blumenfeld, A. Cocoros, N. Eminizer, D. Fehling, L. Feng, A.V. Gritsan, P. Maksimovic, M. Osherson, J. Roskes, U. Sarica, M. Swartz, M. Xiao, Y. Xin, C. You

The University of Kansas, Lawrence, U.S.A.

P. Baringer, A. Bean, C. Bruner, R.P. Kenny III, D. Majumder, M. Malek, W. Mcbrayer, M. Murray, S. Sanders, R. Stringer, Q. Wang

Kansas State University, Manhattan, U.S.A.

A. Ivanov, K. Kaadze, S. Khalil, M. Makouski, Y. Maravin, A. Mohammadi, L.K. Saini, N. Skhirtladze, S. Toda

Lawrence Livermore National Laboratory, Livermore, U.S.A.

D. Lange, F. Rebassoo, D. Wright

University of Maryland, College Park, U.S.A.

C. Anelli, A. Baden, O. Baron, A. Belloni, B. Calvert, S.C. Eno, C. Ferraioli, J.A. Gomez, N.J. Hadley, S. Jabeen, R.G. Kellogg, T. Kolberg, J. Kunkle, Y. Lu, A.C. Mignerey, Y.H. Shin, A. Skuja, M.B. Tonjes, S.C. Tonwar

Massachusetts Institute of Technology, Cambridge, U.S.A.

A. Apyan, R. Barbieri, A. Baty, R. Bi, K. Bierwagen, S. Brandt, W. Busza, I.A. Cali, Z. Demiragli, L. Di Matteo, G. Gomez Ceballos, M. Goncharov, D. Gulhan, Y. Iiyama, G.M. Innocenti, M. Klute, D. Kovalskyi, K. Krajczar, Y.S. Lai, Y.-J. Lee, A. Levin, P.D. Luckey, A.C. Marini, C. Mcginn, C. Mironov, S. Narayanan, X. Niu, C. Paus, C. Roland, G. Roland, J. Salfeld-Nebgen, G.S.F. Stephans, K. Sumorok, K. Tatar, M. Varma, D. Velicanu, J. Veverka, J. Wang, T.W. Wang, B. Wyslouch, M. Yang, V. Zhukova

University of Minnesota, Minneapolis, U.S.A.

A.C. Benvenuti, B. Dahmes, A. Evans, A. Finkel, A. Gude, P. Hansen, S. Kalafut, S.C. Kao, K. Klapoetke, Y. Kubota, Z. Lesko, J. Mans, S. Nourbakhsh, N. Ruckstuhl, R. Rusack, N. Tambe, J. Turkewitz

University of Mississippi, Oxford, U.S.A.

J.G. Acosta, S. Oliveros

University of Nebraska-Lincoln, Lincoln, U.S.A.

E. Avdeeva, R. Bartek, K. Bloom, S. Bose, D.R. Claes, A. Dominguez, C. Fangmeier, R. Gonzalez Suarez, R. Kamalieddin, D. Knowlton, I. Kravchenko, F. Meier, J. Monroy, F. Ratnikov, J.E. Siado, G.R. Snow, B. Stieger

State University of New York at Buffalo, Buffalo, U.S.A.

M. Alyari, J. Dolen, J. George, A. Godshalk, C. Harrington, I. Iashvili, J. Kaisen, A. Kharchilava, A. Kumar, S. Rappoccio, B. Roozbahani

Northeastern University, Boston, U.S.A.

G. Alverson, E. Barberis, D. Baumgartel, M. Chasco, A. Hortiangtham, A. Massironi, D.M. Morse, D. Nash, T. Orimoto, R. Teixeira De Lima, D. Trocino, R.-J. Wang, D. Wood, J. Zhang

Northwestern University, Evanston, U.S.A.

S. Bhattacharya, K.A. Hahn, A. Kubik, J.F. Low, N. Mucia, N. Odell, B. Pollack, M. Schmitt, K. Sung, M. Trovato, M. Velasco

University of Notre Dame, Notre Dame, U.S.A.

N. Dev, M. Hildreth, C. Jessop, D.J. Karmgard, N. Kellams, K. Lannon, N. Marinelli, F. Meng, C. Mueller, Y. Musienko[36], M. Planer, A. Reinsvold, R. Ruchti, N. Rupprecht, G. Smith, S. Taroni, N. Valls, M. Wayne, M. Wolf, A. Woodard

The Ohio State University, Columbus, U.S.A.

L. Antonelli, J. Brinson, B. Bylsma, L.S. Durkin, S. Flowers, A. Hart, C. Hill, R. Hughes, W. Ji, T.Y. Ling, B. Liu, W. Luo, D. Puigh, M. Rodenburg, B.L. Winer, H.W. Wulsin

Princeton University, Princeton, U.S.A.

O. Driga, P. Elmer, J. Hardenbrook, P. Hebda, S.A. Koay, P. Lujan, D. Marlow, T. Medvedeva, M. Mooney, J. Olsen, C. Palmer, P. Piroué, D. Stickland, C. Tully, A. Zuranski

University of Puerto Rico, Mayaguez, U.S.A.

S. Malik

Purdue University, West Lafayette, U.S.A.

A. Barker, V.E. Barnes, D. Benedetti, D. Bortoletto, L. Gutay, M.K. Jha, M. Jones, A.W. Jung, K. Jung, A. Kumar, D.H. Miller, N. Neumeister, B.C. Radburn-Smith, X. Shi, I. Shipsey, D. Silvers, J. Sun, A. Svyatkovskiy, F. Wang, W. Xie, L. Xu

Purdue University Calumet, Hammond, U.S.A.

N. Parashar, J. Stupak

Rice University, Houston, U.S.A.

A. Adair, B. Akgun, Z. Chen, K.M. Ecklund, F.J.M. Geurts, M. Guilbaud, W. Li, B. Michlin, M. Northup, B.P. Padley, R. Redjimi, J. Roberts, J. Rorie, Z. Tu, J. Zabel

University of Rochester, Rochester, U.S.A.

B. Betchart, A. Bodek, P. de Barbaro, R. Demina, Y. Eshaq, T. Ferbel, M. Galanti, A. Garcia-Bellido, J. Han, O. Hindrichs, A. Khukhunaishvili, K.H. Lo, P. Tan, M. Verzetti

Rutgers, The State University of New Jersey, Piscataway, U.S.A.

J.P. Chou, E. Contreras-Campana, D. Ferencek, Y. Gershtein, E. Halkiadakis, M. Heindl, D. Hidas, E. Hughes, S. Kaplan, R. Kunnawalkam Elayavalli, A. Lath, K. Nash, H. Saka, S. Salur, S. Schnetzer, D. Sheffield, S. Somalwar, R. Stone, S. Thomas, P. Thomassen, M. Walker

University of Tennessee, Knoxville, U.S.A.

M. Foerster, G. Riley, K. Rose, S. Spanier, K. Thapa

Texas A&M University, College Station, U.S.A.

O. Bouhali[68], A. Castaneda Hernandez[68], A. Celik, M. Dalchenko, M. De Mattia, A. Delgado, S. Dildick, R. Eusebi, J. Gilmore, T. Huang, T. Kamon[69], V. Krutelyov, R. Mueller, I. Osipenkov, Y. Pakhotin, R. Patel, A. Perloff, D. Rathjens, A. Rose, A. Safonov, A. Tatarinov, K.A. Ulmer

Texas Tech University, Lubbock, U.S.A.

N. Akchurin, C. Cowden, J. Damgov, C. Dragoiu, P.R. Dudero, J. Faulkner, S. Kunori, K. Lamichhane, S.W. Lee, T. Libeiro, S. Undleeb, I. Volobouev

Vanderbilt University, Nashville, U.S.A.

E. Appelt, A.G. Delannoy, S. Greene, A. Gurrola, R. Janjam, W. Johns, C. Maguire, Y. Mao, A. Melo, H. Ni, P. Sheldon, S. Tuo, J. Velkovska, Q. Xu

University of Virginia, Charlottesville, U.S.A.

M.W. Arenton, B. Cox, B. Francis, J. Goodell, R. Hirosky, A. Ledovskoy, H. Li, C. Neu, T. Sinthuprasith, X. Sun, Y. Wang, E. Wolfe, J. Wood, F. Xia

Wayne State University, Detroit, U.S.A.

C. Clarke, R. Harr, P.E. Karchin, C. Kottachchi Kankanamge Don, P. Lamichhane, J. Sturdy

University of Wisconsin - Madison, Madison, WI, U.S.A.

D.A. Belknap, D. Carlsmith, S. Dasu, L. Dodd, S. Duric, B. Gomber, M. Grothe, M. Herndon, A. Hervé, P. Klabbers, A. Lanaro, A. Levine, K. Long, R. Loveless, A. Mohapatra, I. Ojalvo, T. Perry, G.A. Pierro, G. Polese, T. Ruggles, T. Sarangi, A. Savin, A. Sharma, N. Smith, W.H. Smith, D. Taylor, P. Verwilligen, N. Woods

†: Deceased
1: Also at Vienna University of Technology, Vienna, Austria
2: Also at State Key Laboratory of Nuclear Physics and Technology, Peking University, Beijing, China
3: Also at Institut Pluridisciplinaire Hubert Curien, Université de Strasbourg, Université de Haute Alsace Mulhouse, CNRS/IN2P3, Strasbourg, France
4: Also at Skobeltsyn Institute of Nuclear Physics, Lomonosov Moscow State University, Moscow, Russia
5: Also at Universidade Estadual de Campinas, Campinas, Brazil
6: Also at Centre National de la Recherche Scientifique (CNRS) - IN2P3, Paris, France
7: Also at Université Libre de Bruxelles, Bruxelles, Belgium
8: Also at Laboratoire Leprince-Ringuet, Ecole Polytechnique, IN2P3-CNRS, Palaiseau, France
9: Also at Joint Institute for Nuclear Research, Dubna, Russia
10: Also at Ain Shams University, Cairo, Egypt
11: Now at British University in Egypt, Cairo, Egypt
12: Also at Zewail City of Science and Technology, Zewail, Egypt
13: Also at Université de Haute Alsace, Mulhouse, France
14: Also at CERN, European Organization for Nuclear Research, Geneva, Switzerland
15: Also at Tbilisi State University, Tbilisi, Georgia
16: Also at RWTH Aachen University, III. Physikalisches Institut A, Aachen, Germany
17: Also at University of Hamburg, Hamburg, Germany
18: Also at Brandenburg University of Technology, Cottbus, Germany
19: Also at Institute of Nuclear Research ATOMKI, Debrecen, Hungary
20: Also at MTA-ELTE Lendület CMS Particle and Nuclear Physics Group, Eötvös Loránd University, Budapest, Hungary
21: Also at University of Debrecen, Debrecen, Hungary
22: Also at Indian Institute of Science Education and Research, Bhopal, India
23: Also at University of Visva-Bharati, Santiniketan, India
24: Now at King Abdulaziz University, Jeddah, Saudi Arabia

25: Also at University of Ruhuna, Matara, Sri Lanka
26: Also at Isfahan University of Technology, Isfahan, Iran
27: Also at University of Tehran, Department of Engineering Science, Tehran, Iran
28: Also at Plasma Physics Research Center, Science and Research Branch, Islamic Azad University, Tehran, Iran
29: Also at Università degli Studi di Siena, Siena, Italy
30: Also at Purdue University, West Lafayette, U.S.A.
31: Now at Hanyang University, Seoul, Korea
32: Also at International Islamic University of Malaysia, Kuala Lumpur, Malaysia
33: Also at Malaysian Nuclear Agency, MOSTI, Kajang, Malaysia
34: Also at Consejo Nacional de Ciencia y Tecnología, Mexico city, Mexico
35: Also at Warsaw University of Technology, Institute of Electronic Systems, Warsaw, Poland
36: Also at Institute for Nuclear Research, Moscow, Russia
37: Now at National Research Nuclear University 'Moscow Engineering Physics Institute' (MEPhI), Moscow, Russia
38: Also at St. Petersburg State Polytechnical University, St. Petersburg, Russia
39: Also at California Institute of Technology, Pasadena, U.S.A.
40: Also at Faculty of Physics, University of Belgrade, Belgrade, Serbia
41: Also at INFN Sezione di Roma; Università di Roma, Roma, Italy
42: Also at National Technical University of Athens, Athens, Greece
43: Also at Scuola Normale e Sezione dell'INFN, Pisa, Italy
44: Also at National and Kapodistrian University of Athens, Athens, Greece
45: Also at Institute for Theoretical and Experimental Physics, Moscow, Russia
46: Also at Albert Einstein Center for Fundamental Physics, Bern, Switzerland
47: Also at Gaziosmanpasa University, Tokat, Turkey
48: Also at Adiyaman University, Adiyaman, Turkey
49: Also at Mersin University, Mersin, Turkey
50: Also at Cag University, Mersin, Turkey
51: Also at Piri Reis University, Istanbul, Turkey
52: Also at Ozyegin University, Istanbul, Turkey
53: Also at Izmir Institute of Technology, Izmir, Turkey
54: Also at Marmara University, Istanbul, Turkey
55: Also at Kafkas University, Kars, Turkey
56: Also at Istanbul Bilgi University, Istanbul, Turkey
57: Also at Yildiz Technical University, Istanbul, Turkey
58: Also at Hacettepe University, Ankara, Turkey
59: Also at Rutherford Appleton Laboratory, Didcot, U.K.
60: Also at School of Physics and Astronomy, University of Southampton, Southampton, U.K.
61: Also at Instituto de Astrofísica de Canarias, La Laguna, Spain
62: Also at Utah Valley University, Orem, U.S.A.
63: Also at University of Belgrade, Faculty of Physics and Vinca Institute of Nuclear Sciences, Belgrade, Serbia
64: Also at Facoltà Ingegneria, Università di Roma, Roma, Italy
65: Also at Argonne National Laboratory, Argonne, U.S.A.
66: Also at Erzincan University, Erzincan, Turkey
67: Also at Mimar Sinan University, Istanbul, Istanbul, Turkey
68: Also at Texas A&M University at Qatar, Doha, Qatar
69: Also at Kyungpook National University, Daegu, Korea